Friedrich-Schiller-Universität Jena

Biologisch-Pharmazeutische Fakultät

Max-Planck Institut für chemische Ökologie

Arbeitsgruppe Experimentelle Ökologie und Evolution

Generation of auxotrophic *Bacillus subtilis* strains

Masterarbeit

zur Erlangung des Grades eines

Master of Science

vorgelegt von

Ariane Zander

aus Schönebeck

Jena, Februar 2016

Gutachter:

Dr. Christian Kost

Prof. Dr. Johannes Wöstemeyer

SUMMARY

A recently discovered mechanism of how bacterial cells exchange nutrients in cross-feeding interactions is the formation of nanotubes. Cytoplasmic compounds such as proteins and amino acids and possibly even plasmids can be transferred between cells using these structures. It was suggested, that nanotube formation in synthetically engineered cross-feeding interactions involving amino acid auxotrophic *Escherichia coli* cells is triggered by nutrient starvation. Furthermore, nanotube formation was described in *Bacillus subtilis* cells, however, it remains unknown whether nutrients were transported.

The aim of this thesis was to analyze the characteristics of the nanotube formation between cross-feeding *E. coli* and *B. subtilis* cells. For this, cocultures of amino acid auxotrophic *B. subtilis* cells and amino acid overproducing *E. coli* cells should be analyzed. The *B. subtilis* strains, which are auxotrophic for different amino acids should be generated in this thesis.

To generate auxotrophic *B. subtilis* strains, it was first necessary to analyze, which gene deletions generate amino acid auxotrophies. Two different methods were applied to delete the identified target genes, which involved the generation of deletion vectors and LFH-PCR. In both methods, cassettes were created, which contained a resistance cassette flanked by sequences homologous to the sequences flanking the target genes in the genome of *B. subtilis,* which should be knocked out. By transformation of these cassettes into *B. subtilis,* the target gene in the genome of *B. subtilis* should be replaced with the resistance cassette due to homologous recombination.

However, the intended gene deletions were not achieved in this study. Current studies about nanotubes in *E. coli*, which are Gram negative and *B. subtilis*, which are Gram positive differ in several points, e.g. in required cultivation conditions for nanotube formation. Therefore, numerous characteristics of nanotube formation remain unknown, such as potential regulatory mechanisms and specificity of the nanotubes.

ZUSAMMENFASSUNG

Ein Mechanismus für den Austausch von Nährstoffen zwischen Bakterien in cross-feeding Interaktionen ist die Bildung sogenannter Nanotubes. Durch die Nanotubes können cytoplasmatische Elemente wie Proteine und Aminosäuren und möglicherweise auch Plasmide zwischen Bakterienzellen ausgetauscht werden. Es wird vermutet, dass Nährstoffmangel die Bildung der Nanotubes in künstlich hergestellten cross-feeding Interaktionen, die auxotrophe *Escherichia coli* Zellen enthalten, auslöst. Ferner wurden auch Nanotubes bei *Bacillus subtilis* beobachtet, jedoch ist nicht bekannt, ob zwischen diesen Bakterien Nährstoffe ausgetauscht wurden.

Das Ziel dieser Arbeit war es, die Eigenschaften der Nanotubes zwischen *E. coli* und *B. subtilis* Zellen zu analysieren. Dafür sollten Co-Kulturen analysiert werden, die aus *B. subtilis* Zellen bestehen, die auxotroph sind für eine Aminosäure und aus *E. coli* Zellen, die eine andere Aminosäure überproduzieren. Die *B. subtilis* Stämme, die auxotroph sind für jeweils eine Aminosäure, sollten in dieser Arbeit generiert werden.

Dafür wurde zunächst analysiert, welche Gendeletionen in *B. subtilis* zu Auxotrophien führen. Dann wurden zwei verschiedene Methoden angewandt, um die Gendeletionen zu erzielen. Diese Methoden beinhalteten die Herstellung von Deletionsvektoren und LFH-PCR. In beiden Methoden wurden Kassetten hergestellt, die eine Antibiotikum Resistenz Kassette enthielten, die flankiert war von Sequenzen, die homolog waren zu den Sequenzen, die das auszuschaltende Gen flankieren. Anschließend wurde *B. subtilis* mit diesen Kassetten transformiert. Durch homologe Rekombination sollte dann das auszuschaltende Gen durch die Resistenzkassette ersetzt werden.

Jedoch konnten die Gendeletionen in dieser Arbeit nicht erreicht werden. Bestehende Studien zu Nanotubes bei Gram negativen *E. coli* und Gram positiven *B. subtilis* unterscheiden sich in Punkten wie notwendigen Kulturbedingungen für die Bildung von Nanotubes. Daher bleiben zahlreiche Fragen zu den Nanotubes offen, wie zum Beispiel zu den regulatorischen Mechanismen und der Spezifität der Nanotubes.

LIST OF CONTENT

SUMMARY..... i

ZUSAMMENFASSUNG..... ii

I. List of tables.....viii

II. List of figures.....ix

III. List of abbreviations..... x

1. INTRODUCTION..... 1

1.1. Interactions in microbial communities..... 1

1.2. Nutrient cross-feeding..... 2

1.3. Cell-cell transport 3

1.4. Objectives.....5

1.5. Experimental approaches.....5

1.5.1. Introducing *B. subtilis*.....5

1.5.2. Generation of auxotrophic *B. subtilis* strains.....6

1.5.3. Experiments to analyze the nanotube formation by *B. subtilis*.....9

2. MATERIAL AND METHODS.....10

2.1. Media and solutions.....10

2.1.1. LB medium……10

2.1.2. LB agar……...10

2.1.3. Starch agar……10

2.1.4. CSE minimal medium.....10

2.1.5. MC for *B. subtilis*.....11

2.1.6. TFBI and TFBII.....12

2.1.7. TAE buffer.....13

2.1.8. Loading buffer.....13

2.1.9. Lugol solution.....13

2. 2. Strains and plasmids.....14

2.3. Preparation of glycerol stocks.....17

2.4. Determination of target genes.....17

2.5. Gene deletion with deletion vectors.....17

2.5.1. Overview of the gene deletion with deletion vectors.....17

2.5.2. Design of primers.....21

2.5.3. Amplifying the flanking regions of the target genes.....24

2.5.4. Digestion of PCR products.....25

2.5.5. Extraction of plasmids.....26

2.5.6. Digestion of the plasmids.....27

2.5.7. Purification of digested PCR products and plasmids.....27

2.5.8. Ligation of the plasmids with the flanking regions of the target genes.....28

2.5.9. Making *E. coli* chemically competent.....30

2.5.10. Transformation into *E. coli*.....30

2.5.11. Colony-PCR.....31

2.5.12. Digestion of plasmids extracted from potential transformants....32

2.5.14. Sequencing of the plasmids.....33

2.5.15. Transformation of the deletion vectors into *B. subtilis*.....33

2.6. Gene deletion with LFH-PCR.....34

2.6.1. Overview of the gene deletion with LFH – PCR.....34

2.6.2. Design of the primers.....36

2.6.3. Amplification of the flanking regions of the target genes.....36

2.6.4. Amplification of the resistance cassettes.....38

2.6.5. Optimized ratio of resistance cassette to flanking regions in a LFH-PCR.....39

2.6.6. LFH-PCR with all flanking regions.....40

2.6.7. Transformation of LFH-PCR products into *B. subtilis*.....40

2.6.8. Colony PCR with transformants.....41

2.6.9. LFH-PCR with flanking regions of *argH* and *hisD*.....41

2.6.10. Colony PCR with transformants and digestion with *Kpn*I.....42

2.6.11. Growth of transformants in minimal medium with and without amino acid.....42

2.6.12. Sequencing of LFH-PCR products.....43

2.7. GFP- and mKATE-labeling of ordered *B. subtilis* strains.....43

2.7.1. Verifying auxotrophy of ordered *B. subtilis* strains.....43

2.7.2. Transformation with phy-GFP and phy-mKATE.....44

2.7.3. Starch hydrolysis test.....44

3. RESULTS.....45

3.1 Determination of target genes..... 45

3.2. Gene deletion with a deletion vector.....46

3.2.1. Amplification and digestion of the flanking regions of the target genes.....46

3.2.2. Extraction and digestion of plasmids.....47

3.2.3. Ligation and transformation into *E. coli*.....49

3.2.4. Analysis of potential transformants.....49

3.2.5. Transformation of the deletion vectors into *B. subtilis*.....51

3.3. Gene deletion with LFH-PCR.....52

3.3.1. Amplification of regions flanking the target genes and resistance cassettes.....52

3.3.2. LFH-PCR.....53

3.3.3. Transformation of LFH-PCR products into *B. subtilis*.....54

3.3.4. Analysis of the potential transformants.....55

3.3.5. Repeated LFH-PCR with flanking regions of *argH* and *hisD*.....57

3.3.6 Transformation of the purified LFH-PCR products in *B. subtilis*....57

3.3.7. Analysis of the potential transformants of *argH* and *hisD*.....58

3.3.8. Sequencing of LFH-PCR products.....58

3.4. GFP- and mKATE-labeling of ordered *B. subtilis* strains.....59

3.4.1 Verifying auxotrophy of ordered *B. subtilis* strains.....59

3.4.2. GFP- and mKATE-labeling.....60

4. DISCUSSION.....61

4.1. Determination of target genes.....61

4.2. Generation of deletion vectors.....64

4.3. LFH-PCR.....65

4.4. Transformation.....66

4.5. Kanamycin and spectinomycin as selection markers.....66

4.6. Analysis of potential transformants.....67

4.7. Alternative methods for gene deletion in *B. subtilis*.....68

4.8. Labeling of ordered strains.....69

4.9. Comparison of the studies by Dubey and Ben-Yehuda, (2011) and Pande et al., (2015).....71

4.10. The impact of nanotubes.....73

5. CONCLUSION.....75

6. REFERENCES.....77

7. SUPPLEMENTARY……..84

Danksagung……..91

Selbstständigkeitserklärung……92

I. List of tables

Table	Page
Table 1: Components for CSE medium	11
Table 2: Compounds for 10 x MC for *B. subtilis*	11
Table 3: Complete MC for *B. subtilis*	12
Table 4: Compounds for 200 ml TFBI	12
Table 5: Compounds for 50 ml TFBII	12
Table 6: Components of the 6 x loading buffer	13
Table 7: Strains and plasmids used in this study	15
Table 8: Primer for the flanking regions of the target genes	22 – 23
Table 9: PCR to amplify the flanking regions of the target genes	24
Table 10: Double-digestion of the flanking regions of the target genes	26
Table 11: Double-digestion of the plasmids	27
Table 12: Components of the ligation reactions	29
Table 13: Ligation reaction in the fourth attempt of the generation of deletion vectors	29
Table 14: Components of the colony-PCR	31
Table 15: PCR to amplify the flanking regions of the target genes	37
Table 16: PCR to amplify the resistance cassettes	38
Table 17: Components of the LFH-PCR	39
Table 18: Identified target genes	46
Table 19: Concentrations of plasmids and PCR products	49
Table 20: Summary of the results of the colony PCR	50
Table 21: Summary of the analysis of the double-digested plasmids	51
Table 22: Concentrations of purified PCR products resistance cassettes	52
Table 23: Colonies on the transformation plates	54
Table 24: Expected size of the amplified gene regions	56
Table 25: Similarities and differences in the identified target genes	63

Table	Page
Table S1: Restriction enzymes for the amplified flanking regions	85
Table S2: Restriction enzymes used for plasmids	86
Table S3: Double-digestion reactions for testing whether the flanking regions of the target genes were cloned into the plasmids	86
Table S4: Components of the digestion reaction for plasmids pTB233 *lox*-Sp-*lox* with inserted flanking regions of *hisD* and *thrC*	87
Table S5: Primers for the amplification of the flanking regions of the target genes for the LFH-PCR	88
Table S6: Primers for the amplification of the kanamycin- and spectinomycin resistance cassette for the LFH-PCR	89
Table S7: Amplified gene regions to generate template DNA for the LFH-PCR	89
Table S8: Digestion reaction with the restriction enzyme *Kpn*I	90
Table S9: Primers used for sequencing of the LFH-PCR products	90

II. List of figures

Figure	Page
Figure 1: Amino acid cross-feeding in auxotrophic *E. coli*	2
Figure 2: Gene deletion methods deletion vectors and LFH-PCR products	8
Figure 3: Plasmids used in this study	16
Figure 4: Generation of deletion vectors	20
Figure 5: LFH-PCR	35
Figure 6: Agarose gels with plasmids	48
Figure 7: Agarose gel with the LFH-PCR products	53
Figure 8: Agarose gel with colony PCR products	55
Figure 9: Growth of ordered *B. subtilis* strains in minimal medium	59

III. List of abbreviations

aa	Amino acid
Amp	Ampicillin
bla	ß-lactamase
Cat	Chloramphenicol acetyltransferase
CSE	Chromogenic *Salmonella* Esterase
ddH_2O	Double-distilled water
DNA	Deoxyribonucleic acid
dNTP	Deoxynucleotide
ds	downstream
EDTA	Ethylenediaminetetraacetic acid
fw	forward
GFP	Green Fluorescent Protein
LB	Lysogeny Broth
LFH	Long Flanking Homology
MC	Competence medium
mKATE	monomeric far-red *fluorescent protein*
Neo	Neomycin
OD	Optical density
PCR	Polymerase Chain Reaction
rpm	Revolutions per minute
rv	reverse
SAP	Shrimp Alkaline Phosphatase
Sp	Spectinomycin
TFB	Transformation Buffer
T_m	Melting temperature
Tris	Tris (hydroxymethyl) aminomethane
us	Upstream

1. INTRODUCTION

1.1. Interactions in microbial communities

Microorganisms in nature live in communities of many different species (Faust and Raes, 2012). Several interactions have evolved within and/or between species, which have different effects on the interacting partners. These effects can be positive, negative, or neutral.

Competition is an interaction between individuals of the same or different species, which require the same limited resources (Begon et al., 1996). It results in decreasing fitness of at least one partner. Another possible interaction is predation. This is defined as the consumption of one organism by another one, where the attacked organism is still alive. Parasites are considered as predators, too. However, they usually consume only parts of the prey and the attacks are seldom lethal in the short term, but harmful. In contrast to predation, decomposing describes the consumption of dead organic matter. Commensalism describes those interactions, which result in positive effects for one partner and neutral effects for the other partner. An example for commensalism is a host organism, which provides resources or shelter for another organism. This interaction does not result in negative effects for the host organism (Begon et al., 1996). Amensalism is an interaction, where one species excludes the growth of other species (Rastogi and Kishore, 2006). The production of antibiotics by one species, whether or not the other species is present, is an example for amensalism (Begon et al., 1996). Mutualism is the interaction of two species, which results in positive effects for both species (Faust and Raes, 2012). There, the term ‘cooperation’ is often used to describe mutualism between single organisms of the same or different species (Faust and Raes, 2012; Sachs, 2006). Notably, the cooperative act is costly for the concerning organism (Sachs et al., 2004). Cooperative interactions are mostly unidirectional without apparent benefits for the giver. However, this is counterbalanced by cooperative loops, which are formed in natural bacterial communities. Therefore, all involved species gain benefit from the cooperation (Freilich et al., 2011). Furthermore, the term ‘symbiosis’ sometimes is used as synonym for mutualism, but some authors describe all ecological relationships with that term (Faust and Raes, 2012).

1.2. Nutrient cross-feeding

One important example for cooperation is nutrient cross-feeding. This is a cooperation, where metabolites such as vitamins or amino acids are produced and used by the producing organism and used also by other organisms in the environment (Seth and Taga, 2014). Cross-feeding is not restricted to intraspecific interactions, but can also occur between different species (Harcombe, 2010; Pande et al., 2015).

Pande et al. (2014) studied the cross-feeding of amino acids in a synthetic interaction of auxotrophic *Escherichia coli* (Fig. 1). There, the cells of one part of the population were auxotrophic for one amino acid and overproducing another amino acid. The other part of the population was auxotrophic for the amino acid, which was overproduced by the other cells and *vice versa*. They found that this division of labor resulted in an increased fitness of the consortia comprised of auxotrophic and amino acid overproducing cells compared to the prototrophic ancestral strain (wild type). This was explained by the extensive advantage of amino acid auxotrophy, which over-compensated the costs of the overproduction of the respective other amino acid produced by the interacting partner.

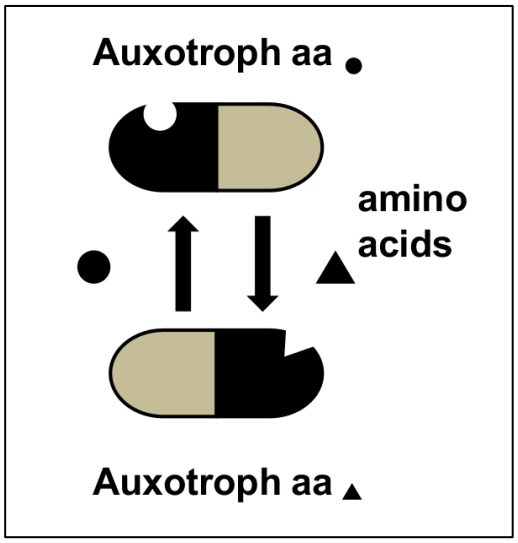

Figure 1: Amino acid (aa) cross-feeding in a synthetic interaction of auxotrophic *E. coli*. Modified after Pande et al. (2014).

The loss of genes, such as in amino acid auxotrophic cells, results in increased fitness compared to a prototrophic wildtype, when the required metabolite is present in the environment of the auxotrophic organism (D'Souza et al., 2014). This is true in the explained amino acid cross-feeding interaction. The fitness benefits can be explained by the saving of costs for the concerning metabolite. Furthermore, a loss of a specific gene results in a saving of costs in the production of the protein, which is required for the biosynthesis of the respective metabolite (D'Souza et al., 2014).

In nature, cross-feeding is of importance because auxotrophies occur frequently in natural bacterial communities. D'Souza et al. (2014) analyzed 949 sequenced genomes of Eubacteria and predicted that 76 % of all Eubacteria are auxotrophic for one to 25 metabolites. Moreover, they predicted that 85 % free-living Eubacteria are auxotrophic for at least one metabolite.

1.3. Cell-cell transport

In cross-feeding interactions, mechanisms of nutrient transport are necessary. Bacteria have evolved different strategies for the transport of ions, metabolites and proteins into and/or out of the cell. They harbor pore forming proteins and carrier proteins in the membrane for active or passive transport through the membrane (Munk et al., 2008). Furthermore, they harbor translocases for the export of proteins. In Gram negative bacteria additional secretion systems allow the transport of proteins and DNA (Deoxyribonucleic acid) through the outer membrane.

However, free diffusion of metabolites in the environment can be detrimental in bacterial interactions (Beveridge, 1999). The metabolites get highly diluted by diffusion. Furthermore, they can be taken up by unsolicited organisms or inactivated by other organisms (Beveridge, 1999; Boyer and Wisniewski-Dyé, 2009). Therefore, different mechanisms of cell-cell transport exist in bacteria. One mechanism is the formation of extracellular vesicles. The vesicles are forced out from the cell surface as globular, bilayered and membranous structures encapsulating periplasm (Beveridge, 1999). Then the vesicles can fuse with the cell surface of other cells to release their contents into the recipient cell. Extracellular vesicles are not only found in Gram negative bacteria but also in Gram positive bacteria as *Bacillus subtilis* and

Staphylococcus aureus (Brown et al., 2014; Lee et al., 2009). Functions of extracellular vesicles are for example cell-cell communication and the transport of virulence factors (Avila-Calderón et al., 2015; Mashburn and Whiteley, 2005).

Another mechanism of cell-cell transport is the formation of channels, as was observed in heterocyst forming filamentous cyanobacteria (Mullineaux et al., 2008). The heterocysts and the vegetative cells have a different and specialized metabolism and they are mutually dependant on each other. Channels are formed between the cells by proteins, which allow the exchange of cytoplasm including sugars and amino acids between the cells.

Pili allow another form of cell-cell transport: DNA and/or proteins are exchanged between cells by type IV secretion systems in the process of plasmid conjugation (Hayes et al., 2010). Furthermore, this system is used by many pathogens to transport toxic effector proteins into the host. In *Myxococcus xanthus*, a bacterium with complex multicellular behaviors, fusion of the outer membranes of different cells allows the exchange of outer membrane proteins and lipids (Ducret et al., 2013).

A further type of cell-cell transport is the formation of nanotubes. This was studied by Pande et al. (2015) in synthetically engineered obligate cross-feeding interactions with different *E. coli* and *Acinetobacter baylyi* strains. They showed that cytoplasmic compounds as proteins and amino acids can be exchanged between cells via nanotubes. The nanotubes consist of membrane derived lipids but the exact structure remains unknown. The transport of cytoplasmic compounds between cells occurs bidirectional. However, it is unknown how specific the exchange of compounds is. In the synthetic interaction two conditions had to be met for the formation of nanotubes: At first, one partner must overproduce one specific amino acid. Second, the other partner must be an *E. coli* cell, auxotrophic for that amino acid. Furthermore, they suggested that nanotube formation is triggered by nutrient starvation. Interestingly, no nanotubes were observed in cross-feeding cocultures that solely consisted of *A. baylyi*.

Additionally, Dubey and Ben-Yehuda (2011) observed the formation of nanotubes between *B. subtilis* cells and between *B. subtilis* and *S. aureus*, which are both Gram positive. Notably, they also observed nanotubes between *B. subtilis* and the Gram negative *E. coli*. There, the nanotubes formed by *E. coli* were thinner than those formed by *B. subtilis* and *S. aureus*. This suggests that nanotubes of Gram positive bacteria

are slightly different from nantotubes of Gram negative bacteria. Furthermore, the nanotubes are different from conjugative pili. In contrast to the study of Pande et al. (2015), the study of Dubey and Ben-Yehuda (2011) showed not only the exchange of cytoplasmic molecules, but also of plasmids between cells via nanotubes. However, Dubey and Ben-Yehuda (2011) did not quantify the formation of nanotubes and neither they did address the question why the nanotubes are formed. The study of Pande et al. (2015) suggests that nutrient starvation triggers the formation of nanotubes.

1.4. Objectives

The aim of this study is to gain more information about the characteristics of the nanotube formation by *B. subtilis*. It will be analyzed whether the nanotube formation by Gram-positive *B. subtilis* cells occurs under similar conditions as described for cross-feeding cultures composed of *E. coli* cells or *E. coli* and *A. baylyi* cells in Pande et al. (2015). Furthermore, one objective is to analyze whether nanotube formation is triggered by nutrient starvation. For coculture experiments with amino acid auxotrophic *B. subtilis* cells and amino acid overproducing *E. coli* cells, auxotrophic *B. subtilis* strains will be generated in this study. For this, genes will be identified, where gene deletion results in amino acid auxotrophy. Then two different methods will be applied to delete those genes. This involves the generation of deletion vectors and LFH-PCR (Long Flanking Homology - Polymerase Chain Reaction).

1.5. Experimental approaches

1.5.1. Introducing *B. subtilis*

B. subtilis belongs to the class Bacilli and to the phylum Firmicutes (Vos et al., 2009). It is an aerobic, Gram-positive, soil dwelling organism and forms endospores. Different strains of *B. subtilis* were used in previous studies, where the strains *B. subtilis* 168 and *B. subtilis* W23 were often used (Zeigler et al., 2008). However, these are domestic laboratory strains and *B. subtilis* NCIB 3610 in contrast, is an ancestral strain (Zeigler et al., 2008). *B. subtilis* NCIB 3610 maintains several characteristics, which are absent in the domestic strains (Konkol et al., 2013). Examples for these characteristics are the

formation of biofilms (McLoon et al., 2011), the ability to swarm and slide (Kearns et al., 2004; Kinsinger et al., 2003), the production of the antibiotic Bacillaene (Butcher et al., 2007), and tryptophan prototrophy (Zeigler et al., 2008). Therefore, *B. subtilis* NCIB 3610 was chosen for this thesis to allow comparisons to natural interactions by *B. subtilis* in the best possible way.

B. subtilis NCIB 3610 harbours a large plasmid (pBS32), which does not occur in the *B. subtilis* strains 168, PY79 or JH642 (Konkol et al., 2013). The plasmid contains the *comI* gene whose gene product ComI inhibits natural competence by interacting with at least one protein of the competence machinery in the membrane (ComGA). Competence is the ability of incorporating free DNA, allowing a genetic transfer process, called transformation (Madigan et al., 2010). Glutamine 12 of ComI is required for the interaction with ComGA. A single base pair change, which disrupts glutamine 12, results in transformation levels similar to strains without plasmid pBS32. Therefore, transformation is possible with the ancestral *B. subtilis* NCIB 3610 *comI*$^{-}$ strain, which was used for this study.

1.5.2. Generation of auxotrophic *B. subtilis* strains

For the analysis of the nanotube formation between cross-feeding *E. coli* and *B. subtilis* cells, amino acid auxotrophic *B. subtilis* strains will be required, which will be generated in this study. The *E. coli* strains, which are required for the cross-feeding interaction are already existent from the study of Pande et al. (2015).

For the generation of auxotrophic *B.subtilis* strains it will be analyzed, which genes have to be knocked out to generate amino acid auxotrophies. Then two different methods will be applied to delete those genes: deletion vectors will be created and LFH-PCR (Yan et al., 2008) will be applied. In both methods cassettes are created, which contain a kanamycin- or spectinomycin resistance cassette flanked by sequences homologous to the sequences flanking the target genes in the genome of *B. subtilis,* which will be deleted (Fig. 2). By transformation of these cassettes into *B. subtilis,* the target gene in the genome of *B. subtilis* is replaced by the antibiotic resistance cassette. This is due to homologous recombination between the homologous sequences in the transformed cassette and in the genome of *B. subtilis*.

In both gene deletion methods the cassettes, which are transformed into *B. subtilis* contain *lox* sites. These sites consist of two 13 bp inverted repeats and a 8 bp core region in the center, which gives site directionality (Sauer, 1987). The *lox* sites are recognized by the Cre recombinase (Cre) from phage P1, which catalyzes the recombination between two *lox* sites (Sauer, 1987). When two *lox* sites are repeated, this recombination leads to excision of the intermediate sequence (Sauer, 1987). In contrast, when two *lox* sites are inverted, the intermediate sequence gets inversed (Sauer, 1987). After recombination of *lox*71 and *lox*66, a *lox*72 site remains in the chromosome. However, *lox*72 has a low binding affinity for Cre, which allows further genetic manipulations (Lambert et al., 2007; Suzuki et al., 2005). The cassettes, which are transformed into *B. subtilis* are designed such that Cre mediates the deletion of the resistance cassette after successful exchange of the target genes with the resistance cassettes. For this, the cells will be transformed with a plasmid containing a *cre* expression cassette.

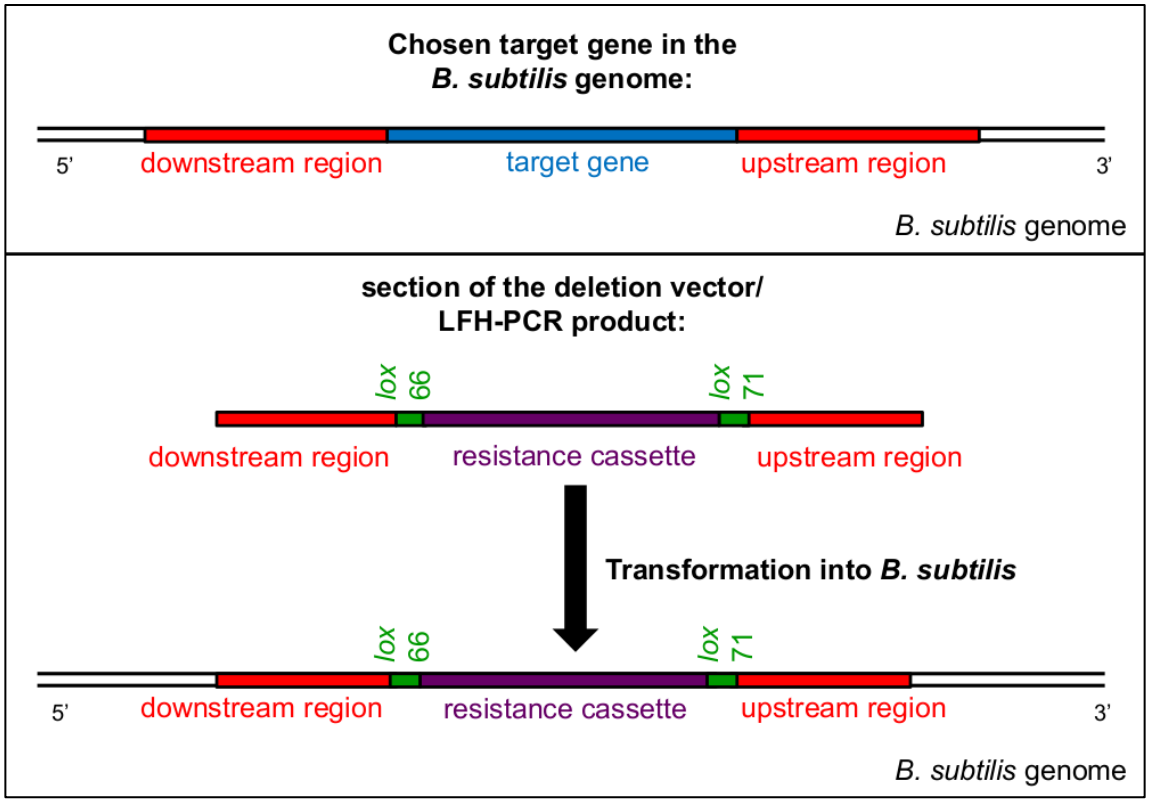

Figure 2: Overview of the gene deletion methods with deletion vectors and LFH-PCR products. The downstream and upstream flanking regions of the target gene in the *B. subtilis* genome (reading frame from 3' to 5') are marked in red, whereas the target gene is marked in blue. Furthermore, a section of the generated deletion vector or the LFH-PCR product, respectively, is shown. These cassettes contain an antibiotic (kanamycin/spectinomycin) resistance cassette flanked by sequences homologous to the sequences flanking the target genes in the genome of *B. subtilis,* which will be deleted. There, the resistance cassette is marked in purple and the *lox* sites are marked in green. The deletion vector or the LFH-PCR product is transformed into *B. subtilis* and the target gene is replaced by the resistance cassette by homologous recombination.

1.5.3. Experiments to analyze the nanotube formation by *B. subtilis*

After verifying the auxotrophy of the generated strains, cross-feeding cocultures will be prepared with *E. coli* cells overproducing an amino acid and *B. subtilis* cells, which are auxotrophic for that amino acid. Growing the cultures in minimal medium with a membrane filter separating the two partners will indicate, whether the exchange of cytoplasmic compounds is indeed contact dependent. The membrane filter does not allow direct cell-cell contact, however, it is permeable for metabolites such as amino acids (Pande et al., 2015). If cross-feeding between *E. coli* and *B. subtilis* is contact dependant, it is expected that no growth occurs, when partners are separated by a membrane filter (Pande et al., 2015). Furthermore, auxotrophic *B. subtilis* strains will be labeled with plasmids encoding a fluorescent protein (phy-GFP, phy-mKATE). Coculture experiments will be conducted, which are comprised of these labeled auxotrophic *B. subtilis* cells and amino acid overproducing *E. coli* cells, which are labeled with another fluorescent marker. Flow cytometry experiments will be performed to quantify both cell types expressing the different fluorescent proteins. The presence of double labeled cells will indicate an exchange of fluorescent proteins via nanotubes (Pande et al., 2015). Moreover, supplementation of the cocultures with the required amino acids will indicate, whether nanotube formation between *E. coli* cells and *B. subtilis* cells is triggered by nutrient starvation. It is expected that nanotube formation will cease after amino acid supplementation, when the nanotube formation is triggered by nutrient starvation.

2. MATERIAL AND METHODS

2.1. Media and solutions

Media and solutions were autoclaved at 121 °C for 15 min prior usage if not stated otherwise.

2.1.1. LB medium

LB medium (Lysogeny broth; Lennox; Carl-Roth, Karlsruhe, Germany) was composed of tryptone (10 g l^{-1}), yeast extract (5 g l^{-1}), and sodium chloride (5 g l^{-1}).

2.1.2. LB agar

LB agar (Lennox; Carl-Roth) contained agar-agar (15 g l^{-1}) and the same components as the LB medium (2.1.1).

2.1.3. Starch agar (Lal and Cheeptham, 2015)

Starch agar was prepared with 1.5 g beef extract (Merck, Darmstadt, Germany), 5 g starch (Sigma-Aldrich, St. Louis, USA), and 6 g agar-agar (Carl-Roth, Karlsruhe, Germany), which was dissolved in 500 ml double-distilled water. The starch agar was heated in a microwave until it started to boil and then autoclaved.

2.1.4. CSE minimal medium (Faires et al., 1999)

For the CSE (Chromogenic *Salmonella* Esterase) minimal medium salt solutions and a glucose solution were prepared (Table 1) and autoclaved. Furthermore, solutions of ammonium citrate, potassium glutamate, and sodium succinate were prepared and sterile filtered with filters of 0.22 µm pore size (Carl-Roth, Karlsruhe, Germany).

Table 1: Components for CSE medium (100 ml; Faires et al., 1999).

Component	Volume (ml)
5 x C salts solution[1]	20.0
Ammonium iron citrate solution ($(NH_4)_5Fe(C_6H_4O_7)2$; 8.40 mM)	1.0
III' salts solution[2]	1.0
Potassium glutamate solution ($C_5H_8KNO_4$; 1.97 M)	2.0
Sodium succinate solution ($C_4H_4Na_2O_4$; 1.11 M)	2.0
Glucose solution ($C_6H_{12}O_6$; 1.01 M)	2.5
ddH_2O	71.5

1: 5 x C salts (200 ml): 4 g monopotassium phosphate, 16 g dipotassium phosphate, 3.3 g ammonium sulfate

2: III' salts (100 ml): 0.0232 g manganese sulfate, 1.23 g magnesium sulfate

2.1.5. MC for *B. subtilis* (iGEM Groningen, 2015)

The compounds for the 10 x MC (Competence Medium; Table 2) were dissolved in 100 ml double-distilled water, sterile filtered with filters of 0.45 µm pore size (Carl-Roth, Karlsruhe, Germany) and stored at – 20 °C. The medium was completed with double-distilled water, magnesiumsulfate, and amino acid when necessary prior to transformation (Table 3).

Table 2: Compounds for 10 x MC for *B. subtilis* (iGEM Groningen, 2015).

Compound	Amount
Dipotassium phosphate (K_2HPO_4)	14.04 g
Monopotassium phosphate (KH_2PO_4)	5.23 g
D-glucose ($C_6H_{12}O_6$)	20.00 g
Tri-sodium citrate solution ($Na_3C_6H_5O_7$; 300 mM)	10.00 ml
Ammonium ferric (III) citrate solution ($(NH_4)_5Fe(C_6H_4O_7)_2$; 83.97 mM)	1.00 ml
Casein hydrolysate	1.00 g
Potassium-glutamate ($C_5H_8KNO_4$)	2.00 g

Table 3: Complete MC for *B. subtilis* (one transformation reaction; iGEM Groningen, 2015).

Compound	Volume (µl)
ddH_2O	1800.0
10 x Competence Medium	200.0
Magnesium sulfate ($MgSO_4$; 1 M)	6.7
Amino acid (10 mM)	40.0

2.1.6. TFBI and TFBII (Hanahan, 1983)

Buffers TFBI (Transformation Buffer) and TFBII were prepared (Table. 4, 5) and adjusted to ph 5.8 with acetic acid in case of TFBI and to pH 6.5 with potassium hydroxide in case of TFBII. Then the buffers were sterile filtered with filters of 0.45 µm pore size.

Table 4: Compounds for TFBI (200 ml; Hanahan, 1983).

Compound	Concentration	Weight / volume
Potassium acetate (CH_3CO_2K)	30 mM	0.59 g
Rubidium chloride (RbCl)	100 mM	2.42 g
Calcium chloride ($CaCl_2$)	10 mM	0.22 g
Glycerol ($C_3H_8O_3$)	16 mM	30.00 ml

Table 5: Compounds for TFBII (50 ml; Hanahan, 1983).

Compound	Concentration	Weight / volume
MOPS (3-(*N*-morpholino) propanesulfonic acid)	10 mM	0.10 g
Rubidium chloride (RbCl)	10 mM	0.06 g
Calcium chloride ($CaCl_2$)	75 mM	0.42 g
Glycerol ($C_3H_8O_3$)	16 mM	7.50 ml

2.1.7. TAE buffer (Odgen and Adamy, 1987)

TAE buffer (Tris-acetate-EDTA, 50 x) was composed of Tris (Tris (hydroxymethyl) aminomethane; 2 M), acetic acid (2 M), and EDTA (Ethylenediaminetetraacetic acid; pH 8.0; 0.5 M). It was not autoclaved prior usage.

2.1.8. Loading buffer

A loading buffer (6 x) was prepared as described in table six (Fermentas, Thermo Fisher Scientific, Waltham, USA). It was not autoclaved prior usage.

Table 6: Components of the 6 x loading buffer (Fermentas, Thermo Fisher Scientific, Waltham, USA).

Component	Concentration (g l^{-1})
Tris-hydrochloride (Tris-HCL; pH 7.6)	1.576
Bromophenol blue	0.3
Xylen Cyanol FF	0.3
Glycerol	6
EDTA	17.5

2.1.9. Lugol solution

Lugol solution is a 1 % aqueous iodine solution, which was obtained from Carl-Roth, Karlsruhe Germany. It was composed of iodine (3.3. g l^{-1}) and potassium iodide (6.7 g l^{-1}). It was not autoclaved prior usage.

2. 2. Strains and plasmids

All strains and plasmids, which were used for this study, are listed in table seven. *B. subtilis* NCIB 3610 and *E. coli* MC1061, which was transformed with plasmids pTB120 *lox*-Neo-*lox*, pTB233 *lox*-Sp-*lox*, phy-GFP, and phy-mKATE, were obtained from the Research Group Terrestrial Biofilms in Jena. The *B. subtilis* strains 1A208, 1A62, 1A543, 1A553, and 1A560 were obtained from the *Bacillus* Genetic Stock Center (Zeigler, 2000). Furthermore, *E. coli* Top Ten was obtained from Invitrogen, Thermo Fisher Scientific, Waltham, USA.

The plasmids pTB120 *lox*-Neo-*lox*, pTB233 *lox*-Sp-*lox*, and phy-GFP are shown in figure three. Plasmid phy-mKATE only differs from phy-GFP in the mKATE sequence. Notably, plasmid pTB120 *lox*-Neo-*lox* harbors the *neo* gene, which encodes a phosphotransferase. The *neo* gene yields resistance in bacteria to various antibiotics, e.g., neomycin and kanamycin (Wright and Thompson, 1999). Due to usage of kanamycin as selection marker in this study, the *neo* gene will be referred to as kanamycin resistance cassette, henceforth.

Table 7: Strains and plasmids used in this study.

Strains and plasmids	Characteristics	Reference
Strains:		
B. subtilis NCIB 3610	pBS32-containing wild type*; comI*$^-$	Konkol et al., (2013)
B. subtilis 1A208	*hisH*$^-$	Nester and Lederberg, (1961)
B. subtilis 1A62	*trpA*$^-$	Whitt and Carlton, (1968)
B. subtilis 1A543	*trpC*$^-$	Whitt and Carlton, (1968)
B. subtilis 1A553	*trpA*$^-$	Whitt and Carlton, (1968)
B. subtilis 1A560	*trpB*$^-$	Whitt and Carlton, (1968)
E. coli MC1061	*araD*139, Δ(*ara*, *leu*)7694, Δ*lacX*74, *galU*$^-$, *galK*$^-$, *hsr*$^-$, *hsm*$^-$, *strA*	Wertman et al., (1986)
E. coli Top Ten	*F- mcrA Δ(mrr-hsdRMS-mcrBC) φ80lacZΔM15 ΔlacX74 nupG rec A1 araD139 Δ(ara-leu)7697 gal E15 galK16 rpsL(*StrR*) endA1 λ*$^-$	Invitrogen, Thermo Fisher Scientific, Waltham, USA
Plasmids:		
pTB120 *lox*-Neo-*lox*	Neo^R, Amp^R cassette	Hölscher et al., (2015)
pTB233 *lox*-Sp-*lox*	Sp^R, Amp^R cassette	Gallegos-Monterrosa, (unpublished)
phy-GFP	Hyper-spank promoter cloned into pGFPrrnB	van Gestel et al., (2014)
phy-mKATE	Hyper-spank promoter cloned into pmKATE2rrnB	van Gestel et al., (2014)

r: resistance cassette

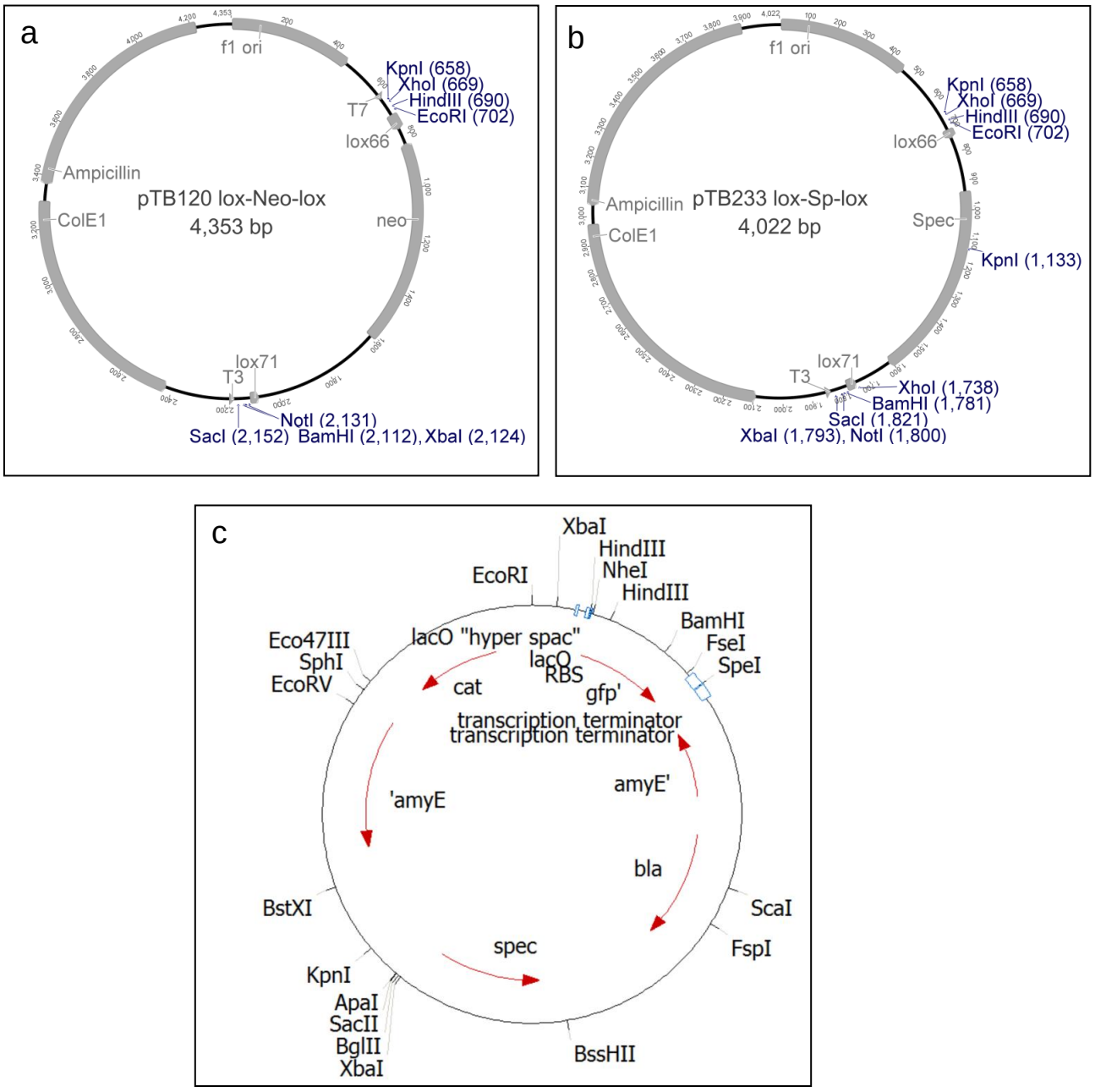

Figure 3: Plasmids used in this study. **a:** Plasmid pTB120 *lox*-Neo-*lox* with a size of 4,353 bp (Hölscher et al., 2015). Genes for ampicillin resistance (Ampicillin) and neomycin resistance (neo) and origins of replication (ColE1, f1 ori) are shown. The *lox*66 site and *lox*71 site as well as binding sites for primer T3 and T7 are presented. Restriction sites are shown with the respective positions in brackets. **b:** Plasmid pTB233 *lox*-Sp-*lox* with the size of 4,022 bp (Gallegos-Monterrosa, R. unpublished). It differs from pTB120 *lox*-Neo-*lox* only in the spectinomycin resistance gene (Spec) and the positions of the restriction sites. **c:** Plasmid phy-GFP with the size of 8,387 bp (van Gestel et al., 2014). Genes coding for ß-lactamase (bla), for spectinomycin resistance (spec), for Chloramphenicol acetyltransferase (cat), and for GFP are shown as well as the *amyE* gene and the *lacO* gene. Transcription terminators, a ribosome binding site (RBS), a *lacO* hyper space, and restriction sites are shown.

2.3. Preparation of glycerol stocks

Glycerol stocks were prepared with all strains, except for *E. coli* Top Ten. For this, overnight cultures were prepared with single colonies in LB medium and incubated at 30 °C under shaking conditions (220 rpm). Then glycerol stocks were prepared with the cultures and glycerol (60 %) in a 1:1 ratio and stored at – 80 °C.

2.4. Determination of target genes

The target genes for generating *B. subtilis* strains that are auxotrophic for one amino acid were determined as described by Bertels et al. (2012). However, there the design and characteristics of auxotrophic *E. coli* genotypes was described, which have biosynthetic pathways of amino acids slightly different from *B. subtilis*.

Genes that catalyze the final step in the biosynthetic pathways of amino acids were considered as target genes that should be deleted. Thereby side effects of the gene deletion, such as deleting central genes important for other pathways, were minimized. When it was not possible to generate auxotrophic strains by deleting the last gene in the biosynthetic pathway, the second last gene was chosen as the target gene. The amino acid biosyntheses pathways of *B. subtilis* were analyzed with the KEGG Pathway database (Kanehisa et al., 2014) and the BsubCyc database (Caspi et al., 2014). Since it was not possible to select *B. subtilis* 3610 as reference strain in these databases, *B. subtilis* 168 was selected.

2.5. Gene deletion with deletion vectors

2.5.1. Overview of the gene deletion with deletion vectors

This paragraph will give an overview of the gene deletion method with deletion vectors and is summarized in figure four. The single working steps will be explained in detail, subsequently.

For the generation of deletion vectors, the plasmids pTB120 *lox*-Neo-*lox* and pTB233 *lox*-Sp-*lox*, which encode a kanamycin and a spectinomycin resistance cassette,

respectively were used. The resistance cassettes within the plasmids were flanked by two different MCSs (multiple cloning sites). The downstream and upstream flanking regions of the target gene in *B. subtilis*, which should be deleted, were cloned into the MCSs of the plasmid. Notably, cloning of the downstream flanking regions of the target genes into the plasmids was performed first. Afterwards, the upstream flanking regions of the target genes were cloned into the plasmids. For this, the downstream and upstream flanking regions of the target genes in *B. subtilis* NCIB 3610 *comI*$^{-}$ were amplified (paragraph 2.5.3.).

For successful transformation it was required that each amplified flanking region was at least 400 bp to 500 bp long (Dubnau, 1993). The reverse primers for the amplification of the downstream flanking regions of the target genes were designed to align with the target genes behind the first 100 bp of the target genes (Fig. 4). Likewise, the forward primers for the amplification of the upstream flanking regions of the target genes were designed to align with the target genes before the last 100 bp of the target genes. This was done to avoid deleting controlling elements for adjacent genes that might be in the region of the last 100 bp, such as promoter regions and inducer– or repressor binding sites (Madigan et al., 2010). Furthermore, the primers harbored restriction sites at the 5' end. Therefore, after amplification of the flanking regions by PCR, the PCR products harbored the artificial restriction site at each end. Then the PCR products were digested with two respective restriction enzymes (double-digestion; paragraph 2.5.4.).

The plasmids pTB120 *lox*-Neo-*lox* and pTB233 *lox*-Sp-*lox* were extracted from *E. coli* MC1061 (paragraph 2.5.5.). Double-digestion was performed with the extracted plasmids, where the restriction enzymes cut within the first Multiple Cloning Site (MCS) of the plasmid (paragraph 2.5.6.). Notably, the same restriction enzymes were used as for the digestion of the amplified downstream flanking regions of the target genes. Accordingly, after double-digestion, the amplified flanking regions of the target genes and the plasmids harbored the same sticky ends, which are short, single stranded overhangs (Madigan et al., 2010). These sticky ends were fused with a DNA ligase (paragraph 2.5.8.). In this way, the downstream flanking regions of the target genes were cloned into the plasmids. Using two different restriction sites at each end of the amplified flanking region assured that the PCR product was cloned with the correct orientation into the MCS within the plasmid. Then the plasmid was transformed into *E. coli* for amplification (paragraph 2.5.10.).

Colony PCR was performed to analyze whether the downstream flanking regions of the target genes were correctly cloned into the plasmids (paragraph 2.5.11.). When this was true, the plasmids were extracted from *E. coli* and the upstream flanking regions of the target genes were cloned into the plasmids similar as the downstream flanking regions. For this, the amplified upstream flanking regions of the target genes and the plasmids were double-digested with different restriction enzymes than used for cloning the downstream flanking regions into the plasmids. Thus it was prevented that the restriction enzymes cut within the already cloned sequences within the plasmids and it allowed cloning of the flanking regions of the target genes into the plasmids in correct orientation.

Then the plasmids were again transformed into *E. coli* for amplification, extracted afterwards and sequenced to analyze whether the flanking regions of the target genes were correctly cloned into the plasmids (paragraph 2.5.14.). For linearization, the plasmids were digested with a restriction enzyme (*Sca*I), which cuts outside of the cloned sequences and the resistance cassettes and then were transformed into *B. subtilis* NCIB 3610 *comI*$^{-}$ (paragraph 2.5.15.). Hypothetically, homologous recombination between the homologous sequences within the plasmids and the *B. subtilis* genome exchanged the target genes in the *B. subtilis* genome with the resistance cassettes of the plasmids. Growing the transformed cells on LB agar with kanamycin or spectinomycin, respectively allowed positive selection of the resistant cells.

The method of generating deletion vectors was performed four times. Experimental conditions slightly differed between the four attempts as will be pointed out in the respective paragraph. Notably, in case of *trpC* the upstream flanking region was cloned first into the plasmids. This was necessary, because the downstream flanking region of *trpC* harbors an *Xba*I restriction site and the *Xba*I restriction enzyme was used for digestion of the amplified upstream region of *trpC*. Therefore, the downstream flanking region of *trpC* would have been restricted, if the downstream flanking region was cloned first into the plasmids.

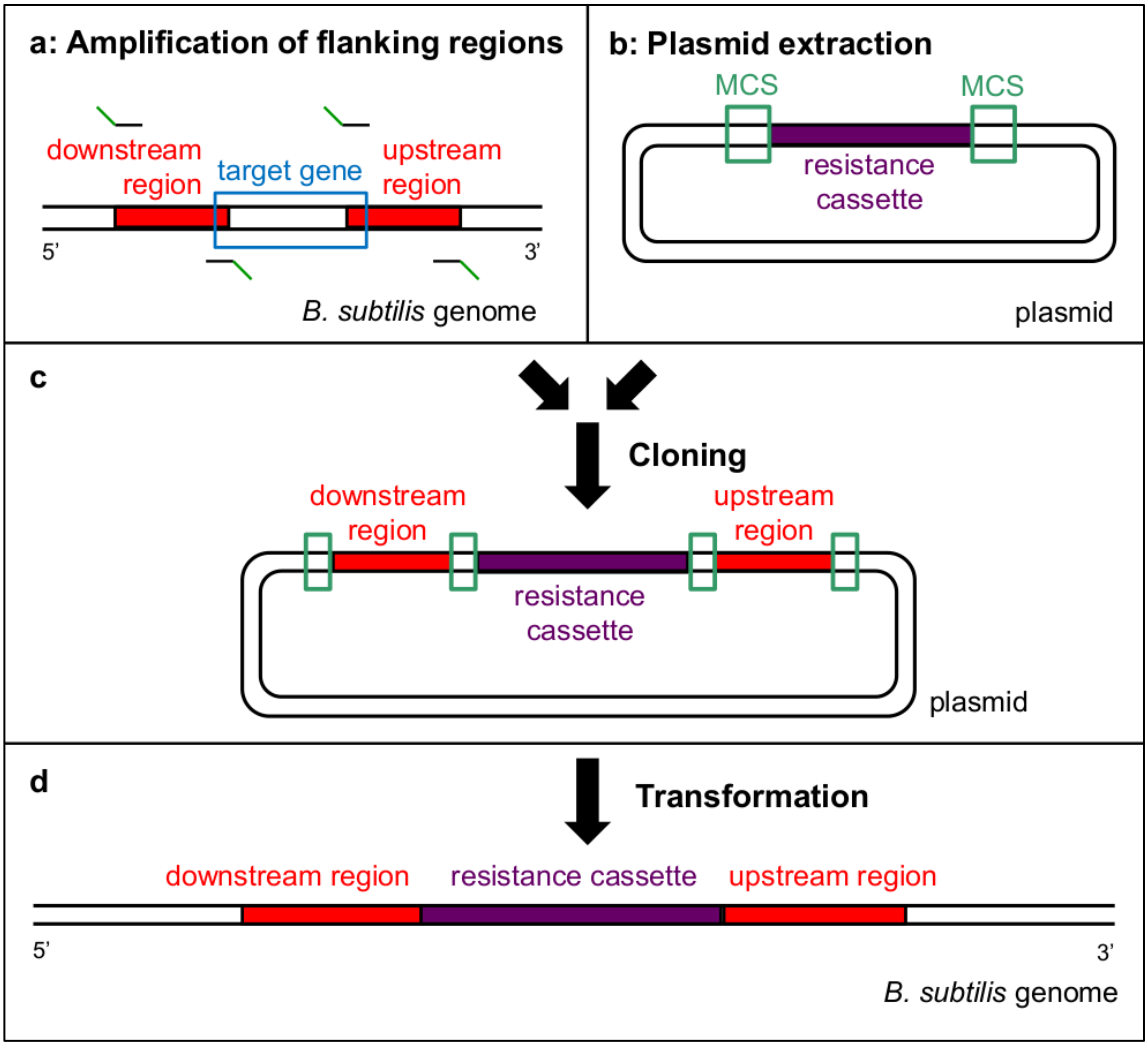

Figure 4: Overview of the generation of deletion vectors to generate amino acid auxotrophic *B. subtilis* strains. **a:** The flanking regions of the target gene in the *B. subtilis* genome (reading frame from 3' to 5') are amplified by PCR. **b**: The plasmid with a resistance cassette (resistance for kanamycin or spectinomycin) are extracted from *E. coli* **c:** The flanking regions of the target gene are cloned into the MCSs of the plasmids. **d:** The deletion vector is transformed into *B. subtilis* and the target gene is replaced by the resistance cassette by homologous recombination. Flanking regions of the target gene are marked in red, the target gene is marked in blue, the resistance cassette is marked in purple, and the Multiple Cloning Sites (MCS) are marked in turquoise. Primers are indicated as black lines and the sequences, which are added to the primers, are marked in green.

2.5.2. Design of primers

Forward and reverse primers for the flanking regions of each target gene were designed so that each amplified region was 550 bp to 770 bp long. The sequences of the target gene regions were downloaded from the BIOCYC Database collection (Caspi et al., 2014). For this, the genome of *B. subtilis* 168 was used as reference genome because it was not possible with *B. subtilis* NCIB 3610 *comI*$^{-}$. Primers were designed using the webpage Primer 3 (Koressaar and Remm 2007; Untergasser et al. 2012). Subsequently, restriction sites were added to the 5' ends of the primers (Table 8). Furthermore, one to three extra base pairs were added to the 5' ends of the primers to allow complete digestion with the respective restriction enzymes (Cleavage Close to the End of DNA Fragments, 2015). Different restriction sites were used for the different flanking regions of the target genes to allow correct cloning of the flanking regions into the plasmids pTB120 and pTB233 in two steps. Additional primers were designed, which bind outside of the 550 bp to 770 bp long flanking regions of the target genes. No restriction sites were added to those additional primers.

Table 8: Primers for the amplification of the flanking regions of the target genes with added restriction sites.

Amino acid	Target gene	Primer name	Restriction	site	Sequence (5' to 3')
arginine	*argH*	argH d_fw_SalI	*Sal*I	GTCGAC	TTCGTCGACAAGTCGATCCTTCCGAAGCG
		argH d_rv_EcoRI	*Eco*RI	GAATTC	TGTGAATTCCACCGGATTCAAACAGGTGG
		argH u_fw_XbaI	*Xba*I	TCTAGA	GCCTCTAGACGGATTTTCAACTCTTCTTCTGC
		argH u_rv_SacI	*Sac*I	GAGCTC	TGAGCTCTGACGGTGTTTCCTACTCGC
		argH o_fw			ATGCTTCTTTCATGTCGCCG
		argH o_rv			TTCGGCATTATCTCGACCGC
histidine	*hisD*	hisD d_fw_HindIII	*Hind*III	AAGCTT	TGTAAGCTTCGCCGATCATTTACAGCATCC
		hisD d_rv_EcoRI	*Eco*RI	GAATTC	TCGGAATTCAGCCTTTGAAGAACATGCCG
		hisD u_fw_XbaI	*Xba*I	TCTAGA	GCTTCTAGAAAATTTCGCCGTGTAGCTGC
		hisD u_rv_SacI	*Sac*I	GAGCTC	GGAGCTCGGATGTCATGCTGGAGGAGG
		hisD o_fw			ACTCCCGGCAAAATGAAAGC
		hisD o_rv			CCGGATATTTGAAGAAGCGGC
lysine	*lysA*	lysA d_fw_HindIII	*Hind*III	AAGCTT	GTCAAGCTTCAGCCGGTGTTAAAGATGCG
		lysA d_rv_EcoRI	*Eco*RI	GAATTC	GTAGAATTCTTTGTCGAAAACGGTGAGGC
		lysA u_fw_XbaI	*Xba*I	TCTAGA	ATCTCTAGATAGAGAGCATCCACACCTCC
		lysA u_rv_SacI	*Sac*I	GAGCTC	TGAGCTCGCATATCCCGATCATCCTGC
		lysA o_fw			CCGGATTGAATGTTGAGACCC
		lysA o_rv			CCGATCTGGTTTCTCTTTGTGC

Table 8 continued

tyrosine	*tyrA*	tyrA d_fw_SalI	*Sal*I	GTCGAC	CCAGTCGACGGTCCCGAGATTTATGGGGC
		tyrA d_rv_EcoRI	*Eco*RI	GAATTC	CGTGAATTCGCATCAGTATCACGAATATCCGC
		tyrA u_fw_XbaI	*Xba*I	TCTAGA	AAGTCTAGATTCCGATAATCCGTTTGCCG
		tyrA u_rv_SacI	*Sac*L	GAGCTC	TGAGCTCCGGAATTGCTGACGAGAACC
		tyrA o_fw			GCTGTTTGGAACCATCGCG
		tyrA o_rv			TCCTTCTCGTGTCCTTGTCG
phenylalanine	*pheA*	pheA d_fw_HindIII	*Hind*III	AAGCTT	CGTAAGCTTAAATCACCGCTGACAGGAGG
		pheA d_rv_EcoRI	*Eco*RI	GAATTC	CTAGAATTCATTGATTCCAGGGGCCATGC
		pheA u_fw_XbaI	*Xba*I	TCTAGA	CATTCTAGAGTAAGCAACATGTTCGGCGC
		pheA u_rv_SacI	*Sac*I	GAGCTC	CGAGCTCCGGAATGGGTGTTGATGAAGC
		pheA o_fw			TTTGGCAGGCATACAACAGC
		pheA o_rv			ATTACACGCGATCCAGACGG
tryptophan	*trpC*	trpC d_fw_HindIII	*Hind*III	AAGCTT	ATCAAGCTTTAGGCGTGTGATGCTATCCG
		trpC d_rv_EcoRI	*Eco*RI	GAATTC	ACCGAATTCTTGTCAATGAACATGGGGCG
		trpC u_fw_XbaI	*Xba*I	TCTAGA	GTCTCTAGACAGCGCCTCCTTAAATGAACG
		trpC u_rv_SacI	*Sac*I	GAGCTC	TGAGCTCGCGCTGATGTTTTAGAGGAGC
		trpC o_fw			ACTTTCCGCCAAAATCACCG
		trpC o_rv			TTTTGTGAAGGCAATGCGGG
threonine	*thrC*	thrC d_fw_HindIII	*Hind*III	AAGCTT	AGGAAGCTTTCCTTGGACATGATCGCAGC
		thrC d_rv_PstI	*Pst*I	CTGCAG	GACCTGCAGCTGAAAGATCCGAACACAGCG
		thrC_u_fw_BamHI-HF	*Bam*HI	GGATCC	CTGGGATCCGCCTTCCGTTTTGACATGAAGC
		thrC u_fw_NotI-HF	*Not*I	GCGGCCGC	TGCGGCCGCTGCTTCCTGACCATCATCCG
		thrC o_fw			ATATGCGCCCTTCATCTCGG
		thrC o_rv			TGAACGTGGATCTGGAAGACG

Abbreviations in the primer names: d: downstream. u: upstream. fw: forward. rv: reverse. Added restriction sites in blue. Spacer sequences in red.

2.5.3. Amplifying the flanking regions of the target genes

The flanking regions of the target genes were amplified in a 15 µl colony PCR, using the Phusion High-Fidelity Polymerase (Thermo Fischer Scientific, Waltham, USA; Table 9). There, the template was 1 µl of the glycerol stock of *B. subtilis* NCIB 3610 *comI*$^-$ suspended in 50 µl autoclaved, double-distilled water. For each flanking region, the reaction was prepared in four 15 µl reactions, which were pooled afterwards to gain 60 µl PCR product. Melting temperatures (T_m) were calculated using the webpage T_m calculator of Thermo Fisher Scientific (T_m calculator, 2015). Furthermore, negative controls without template were prepared.

Table 9: Components of the colony PCR for the amplification of the flanking regions of the target genes for the gene deletion with a deletion vector.

Component	**Volume (µl)**
5 x Phusion High-Fidelity Buffer (Thermo Fisher Scientific, Waltham, USA)	3.00
dNTPs (10 mM; Kapa Biosystems, Wilmington, USA)	0.30
Forward primer[1] (10 pmol µl^{-1})	0.75
Reverse primer[1] (10 pmol µl^{-1})	0.75
Template[2]	1.00
Phusion High-Fidelity Polymerase	0.15
ddH_2O (autoclaved)	9.00

1: primers shown in table 8; 2: 1 µl glycerol stock of *B. subtilis* NCIB 3610 *comI*$^-$ in 50 µl autoclaved ddH_2O. dNTP: deoxynucleotide

The PCR program was as follows:

Initial denaturation:	98 °C for 30 s	
Denaturation:	98 °C for 10 s	x 40
Annealing:	65 °C for 15 s	
Extension:	72 °C for 30 s	
Final extension:	72 °C for 5 min	
Holding:	10 °C ∞	

Finally, the PCR products were analyzed in a 1 % agarose gel. For this, 0.6 g agarose was dissolved in 60 ml TAE buffer by heating the solution in a microwave. Then 3 µl ethidium bromide solution (10 mg ml^{-1}; Sigma-Aldrich, St. Louis, USA) was added and the gel was cast. After the agarose gel had solidified, 10 µl PCR product with 2 µl loading buffer was loaded into the agarose gel. Furthermore, 6 µl Gene Ruler^{TM} 1 kb Plus DNA ladder (Fermentas, Thermo Fisher Scientific, Waltham, USA) was loaded into the gel. The agarose gel was run at 130 V for 40 min.

2.5.4. Digestion of PCR products

A double-digestion of the PCR products was performed using the corresponding FastDigest restriction enzymes (Thermo Fisher Scientific, Waltham, USA; Table 8). PCR products were not purified prior digestion to avoid unwanted loss of the products during that process. The composition of the double-digestion reactions slightly differed between the four attempts of generating deletion vectors (Table 10). Reactions were incubated at 37 °C in a heating block. Incubation times were set according to the manual by Thermo Fisher Scientific considering possible star activity (Table S1). Star activity is the cleaving of sequences, which are similar but unidentical to the restriction sites (Star activity. New England BioLabs, 2016). During the fourth attempt of generating deletion vectors, all digestion reactions were incubated for the same time, because for these restriction enzymes no star activity was observed with 90 min incubation time (Gallegos-Monterrosa, 2015). The restriction enzyme, which needed a longer incubation time, was added first to the reaction and after the respective incubation time the second restriction enzyme was added. For thermal inactivation of restriction enzymes all reactions were incubated at 80 °C for 10 min. However, for *Pst*I thermal inactivation was not possible. Since the digested PCR products were purified afterwards, thermal inactivation of the restriction enzymes was not essential to the method.

Table 10: Reactions of the double-digestion of the amplified flanking regions in attempt (A) one, two, three, and four of generating deletion vectors.

Component	For A1, A2, A3 Volume (µl)	For A4 Volume (µl)
PCR-product (amplified flanking region)	10	12
10 x FastDigest Buffer (Thermo Fisher Scientific, Waltham, USA)	4	3
FastDigest restriction enzyme	2 of each	1 of each
ddH_2O (autoclaved)	22	13

2.5.5. Extraction of plasmids

Single colonies of *E. coli* MC1061 with plasmids pTB120 *lox*-Neo-*lox* and with pTB233 *lox*-Sp-*lox*, respectively were inoculated in 4 ml LB in a 50 ml falkon tube. *E. coli* with the plasmid pTB120 *lox*-Neo-*lox* was grown with additional kanamycin (25 µg ml^{-1}) and *E. coli* with the plasmid pTB233 *lox*-Sp-*lox* was grown with additional spectinomycin (100 µg ml^{-1}). The cultures were incubated at 37 °C for about 16 h under shaking conditions (220 rpm). Plasmid extraction was performed with these cultures using the GeneJET Plasmid Miniprep Kit (Thermo Fisher Scientific, Waltham, USA) following the manufacturer's instructions. For this, the cultures were centrifuged and the pellets of bacterial cells were resuspended with a solution containing RNAse A. The cells were lysed by alkaline lysis, what liberates plasmid DNA (Birnboim and Doly, 1979). Then the lysate was neutralized with a neutralization solution and loaded onto a silica membrane (Vogelstein and Gillespie, 1979). Cell debris was pelleted by centrifugation and the resulting supernatant was washed with the washing solution in several centrifugation steps. All centrifugations were performed at 13,000 x g. Different from the manufacturer's instructions the plasmid DNA was eluted with 50 µl autoclaved, double-distilled water instead of elution buffer to avoid interference of the elution buffer in the ligation reactions. Prior to elution of plasmid DNA, samples were incubated at 60 °C to increase the concentration of the eluted plasmid DNA. The purified plasmid DNA was stored at – 20 °C.

2.5.6. Digestion of the plasmids

A double-digestion of the plasmids pTB120 *lox*-Neo-*lox* and pTB233 *lox*-Sp-*lox* was performed using FastDigest restriction enzymes (Thermo Fisher Scientific) similar as described in paragraph 2.5.4. Each plasmid was digested with different restriction enzymes to match those used for the amplified flanking regions of the target genes. The composition of the reactions slightly differed between the four attempts of generating deletion vectors, because different volumes of plasmid DNA were applied due to differing DNA concentrations (Table 11).

After double-digestion, the plasmids were treated with Shrimp Alkaline Phosphatase (SAP; Fermentas Life Sciences). This enzyme dephosphorylates the plasmid to avoid recircularization. Each double-digestion reaction was supplied with 2 µl SAP and incubated at 37 °C for 30 min. The reaction was stopped by incubation at 65 °C for 15 min. The digested plasmids were analyzed in a 1 % agarose gel as described in paragraph 2.5.3.

Table 11: Reactions of the double-digestion of the plasmids pTB120 *lox*-Neo-*lox*, pTB233 *lox*-Sp-*lox* and pTB233 *lox*-Sp-*lox* with the inserted downstream flanking regions of the target genes in attempt (A) one, two, three, and four of generating deletion vectors.

Compound	**Volume (µl)**		
	A1	**A2, A3**	**A4**
Plasmid DNA	20	10	12
10 x FastDigest buffer	4	5	3
FastDigest restriction enzyme	2 of each	2.5 of each	1 of each
ddH_2O	12	30	13

2.5.7. Purification of digested PCR products and plasmids

The digested PCR products and plasmids were purified using the PureLink PCR-Purification Kit or the PureLink Quick Gel extraction and PCR purification Kombo Kit (Invitrogen, Thermo Fisher Scientific, Waltham, USA) following the manufacturer's protocol. There, the DNA samples were loaded onto a silica-based membrane,

which selectively bound double-stranded DNA. Binding Buffer (B2) was used for PCR products and Binding Buffer (B3) for plasmids. Then the samples were washed with Washing Buffer. After addition of the Washing Buffer, the samples were incubated at room temperature for 1 min. Elution was performed with autoclaved, double-distilled water instead of elution buffer and incubation was done at 60 °C for 2 min before elution. PCR products were eluted with 25 µl autoclaved, double-distilled water and plasmids were eluted with 50 autoclaved, double-distilled water.

In the fourth attempt of generating deletion vectors, the High Pure PCR Product Purification Kit (Roche, Basel, Switzerland) was used following the manufacturer's protocol. There, the DNA samples were loaded into a filter tube where it bound selectively to glass fibers. The samples were washed with Washing Buffer in several centrifugation steps and the DNA was eluted with 20 µl elution buffer consisting of a low salt solution. The elution centrifugation step was performed with 8000 x g to avoid glass fibers contaminating the purified DNA samples.

Concentrations of the DNA samples were measured with the Nanovue (GE Healthcare, Chalfont St Giles, UK). For this, 2 µl autoclaved, double-distilled water was used as reference and 2 µl DNA sample was applied for the measurement. Measured concentrations always were corrected with the A260 nm to A280 nm ratios as described in Glasel (1995).

2.5.8. Ligation of the plasmids with the flanking regions of the target genes

The double-digested and purified amplified flanking regions of the target genes were ligated with the double-digested and purified plasmids. In the first and second attempt of generating deletion vectors, only the downstream flanking regions were ligated with the plasmids. In the third and fourth attempt, additionally the upstream flanking regions were ligated with the plasmid that already contained the corresponding downstream region. The T4 DNA ligase and 10 x T4 DNA ligase buffer (Thermo Fisher Scientific, Waltham, USA) were used for the ligation reactions (Table 12, 13).

Different ratios of plasmids to flanking region of the target genes were tested in the first attempt of generating deletion vectors: 1:7 and 1:15 and 1:20. The necessary amounts of plasmid DNA and PCR product for the ligation were calculated using the webpage

Ligation Calculator (Krauss and Eggert, 2015). Subsequently, only the ratio of plasmid to flanking region of 1:20 was applied. Negative controls with the digested plasmids without PCR product were prepared to test for recyclization of the plasmid. The ligation reactions were incubated at room temperature for 2 h. However, in the fourth attempt of generating deletion vectors, the ligation reactions were incubated at 18 °C for 1.5 h. Then the ligase was heat inactivated by incubation at 65 °C for 10 min.

Table 12: Components of the ligation reaction in attempt (A) one, two, and three of generating deletion vectors.

Compound	**Amount**
Plasmid DNA: pTB120 *lox*-Neo-*lox* or pTB233 *lox*-Sp-*lox*	20 ng to 100 ng
Amplified flanking region (PCR product)	7:1 and 15:1 and 20:1 ratio over plasmid DNA in A1; 20:1 ratio over plasmid DNA in A2, A3, A4
T4 DNA ligase	1 µl
10 x T4 DNA ligase buffer	2 µl
ATP (10 mM working stock; Thermo Fisher Scientific, Waltham, USA)	1 µl
ddH_2O	to 20 µl

Table 13: Components of the ligation reaction in the fourth attempt of the generation of deletion vectors.

Compound	**Volume (µl)**
Plasmid DNA: pTB120 *lox*-Neo-*lox* or pTB233 *lox*-Sp-*lox* or pTB233 *lox*-Sp-*lox* with 1st insert	 2 2 1
Amplified flanking region (PCR product)	7
T4 DNA ligase	1
10 x T4 DNA ligase buffer	2
ddH_2O	5

2.5.9. Making *E. coli* chemically competent

For transformation of the ligation products into *E. coli* Top Ten, the cells had to be made competent. For this, a modified Rubidium-chloride method was applied to obtain chemically competent *E.coli* cells (NEB. Rubidium Chloride Method, expired). *E. coli* Top Ten was streaked on LB agar plates and incubated at 30 °C. The next day, a single colony was inoculated in 2 ml LB medium and incubated at 30 °C under shaking conditions (220 rpm) overnight. A subculture was prepared in an Erlenmeyer flask using 100 ml LB medium with additional $MgSO_4$ (final concentration 20 mM) and 1 ml of the overnight culture. The subculture was grown to an optical density (OD; 600 nm) of 0.4. Then it was centrifuged at 5,000 rpm for 5 min at 4 °C, the supernatant was discarded and the pellet was resuspended in 40 ml TFBI Buffer. After incubation on ice for 5 min the culture was centrifuged at 5,000 rpm for 5 min at 4 °C. The resulting supernatant was discarded and the pellet was resuspended in 10 ml TFBII buffer and incubated on ice for 50 min. Finally, the cells were aliquoted in pre-cooled Eppendorf tubes and the competent cells were stored at – 80 °C.

2.5.10. Transformation into *E. coli*

For transformation, 50 µl of competent *E. coli* Top Ten cells were mixed with 10 µl of the ligation reaction. The cells were incubated on ice for 15 min and then heat shocked at 42 °C for 45 s. After addition of 1 ml LB medium, the cells were incubated at 37 °C under shaking conditions (220 rpm). The transformation cultures with pTB120 *lox*-Neo-*lox* were plated on LB agar with kanamycin (25 µg ml^{-1}) and cultures with pTB233 *lox*-Sp-*lox* were plated on LB agar with spectinomycin (50 µg ml^{-1}). However, in the fourth attempt of generating deletion vectors, all cultures were plated on LB agar with ampicillin (100 µg ml^{-1}).

2.5.11. Colony-PCR

To analyze whether the flanking regions of the target genes were inserted into the plasmids, a colony-PCR was performed. For this, single colonies from the plates with the transformation cultures were replica-streaked on LB agar with the respective antibiotic. Colonies with pTB120 *lox*-Neo-*lox* were streaked on LB agar with kanamycin (25 µg ml^{-1}) and colonies with pTB233 *lox-Sp-lox* on LB agar with spectinomycin (50 µg ml^{-1}) or both were streaked on LB agar with ampicillin (100 µg ml^{-1}). Then, a section of that colony was put into a PCR tube and microwaved at maximum power for 1 min to lyse the potential transformants. Finally, the PCR mix, which included a JumpStart Taq ready mix by Sigma-Aldrich (St. Louis, USA), primers and autoclaved, double-distilled water, was added to the cells in the PCR tube (Table 14). There, the same primers were used as for the amplification of the flanking regions of the target genes.

Table 14: Components of the colony-PCR to analyze, whether the flanking regions of the target genes were cloned into the plasmid pTB120 *lox*-Neo-*lox* or pTB233 *lox-Sp-lox.*

Component	Volume (µl)
JumpStart Taq ready mix	12.50
Forward primer[1] (10 pmol $µl^{-1}$)	0.75
Reverse primer[1] (10 pmol $µl^{-1}$)	0.75
ddH_2O (autoclaved)	6.00

1: same primers as used for the PCR for amplifying the flanking regions of the target genes (Table 8)

The PCR program was as follows:

Initial denaturation:	95 °C for 6 min	
Denaturation:	95 °C for 30 s	
Annealing:	65 °C for 30 s	x 30
Extension:	72 °C for 1 min	
Final extension:	72 °C for 10 min	
Holding:	10 °C ∞	

Finally, the colony-PCR products were analyzed in a 1 % agarose gel as described in paragraph 2.5.3.

2.5.12. Digestion of plasmids extracted from potential transformants

Plasmids were extracted from the potential transformants, which showed a band in the colony PCR as described in paragraph 2.4.5. Furthermore, glycerol stocks were prepared with the potential transformants as described in paragraph 2.3.

The extracted plasmids were double-digested as described in paragraph 2.5.6., to liberate the flanking regions of the target genes, which were cloned into the plasmids. Reactions were prepared as described in table S3. There, the same restriction enzymes were used as for the double-digestion of the plasmids and PCR products prior ligation. The digested plasmids were analyzed in a 1 % agarose gel as described in paragraph 2.5.3.

2.5.14. Sequencing of the plasmids

Plasmids pTB233 *lox*-Sp-*lox* with inserted flanking regions of *hisD*, *tyrA* and *thrC* were diluted to 60 ng μl^{-1} to 100 ng μl^{-1} and sequenced with primers T3 and T7 by Eurofins Genomics (Ebersberg, Germany). The sequencing results were analyzed using the software Geneious® 6.1.8. (Biomatters, New Zealand; Kearse et al., 2012). For this, the sequencing results were aligned with the respective sequence of the target gene regions.

2.5.15. Transformation of the deletion vectors into *B. subtilis*

The plasmids pTB233 *lox*-Sp-*lox* that contained the flanking regions of *hisD* and *thrC* were transformed into *B. subtilis* NCIB 3610 *comI*$^-$. Prior to transformation, the plasmids were digested with the FastDigest restriction enzyme *Sca*I (Table S4), which cuts the plasmid outside of the cloned flanking regions of the target genes. The reactions were incubated in a heating block at 37 °C for 30 min. Then the restriction enzyme was heat inactivated by incubation at 65 °C for 10 min. Subsequently, 2 µl of SAP was added to each reaction and the reactions were incubated at 37 °C for 30 min. The reaction was stopped by incubation at 65 °C for 15 min. Digested plasmids were purified and concentrations of the plasmid DNA were measured as described in paragraph 2.5.7.

For transformation, a single colony of *B. subtilis* 3610 com I$^-$ was inoculated in 2 ml LB medium and incubated at 30 °C for 18 h under shaking conditions (220 rpm). The competence medium was supplemented with histidine and threonine, respectively. Then the media were inoculated with 50 µl of the culture and incubated at 37 °C for 4 h under shaking conditions (220 rpm). Subsequently, 400 µl of each culture was added to a new tube and the digested and purified plasmid DNA (1 µg) was added. The plasmid pTB233 *lox*-Sp-*lox* with flanking regions of *hisD* was added to the culture grown with histidine and the plasmid pTB233 *lox*-Sp-*lox* with flanking regions of *thrC* was added to the culture grown with threonine. The cultures were incubated at 37 °C for 2 h under shaking conditions (220 rpm). Then they were plated on LB agar with spectinomycin (100 µg ml^{-1}) and the focal amino acid (200 µM) and incubated at 37 °C for four days.

2.6. Gene deletion with LFH-PCR

2.6.1. Overview of the gene deletion with LFH – PCR

This paragraph will give an overview of the LFH-PCR, which was used for gene deletion. The gene deletion with LFH-PCR products is summarized in figure five. Following paragraphs will give more details about the individual working steps.

In this method LFH-PCR was used as described by Yan et al. (2008). The downstream and upstream flanking regions of the target genes were amplified by PCR (paragraph 2.6.3.). Similar to the gene deletion with deletion vectors, primers were designed to amplify flanking regions of 500 bp to 700 bp. However, the primers, which aligned within the ends of the target genes, were designed to contain an additional sequence at the 5' end, which was the *lox*66 site for the downstream flanking regions and the *lox*71 site for the upstream flanking regions of the target genes. The *lox* sites were added such, that they had the same direction in the LFH-PCR product to allow gene deletion with the Cre/*lox* system later on. By amplification of the flanking regions, the *lox* sites were added to the flanking regions.

Furthermore, the resistance cassettes for kanamycin and spectinomycin, respectively were amplified by PCR (paragraph 2.6.4.). For this, the forward primer contained the *lox*71 site and the reverse primer contained the *lox*66 site at the 5' end. Consequently, the amplified resistance cassettes contained a *lox* site at each end. In the first step of the LFH-PCR, the amplified resistance cassettes were fused with the amplified flanking regions of the target gene due to their homologous ends (paragraph 2.6.5.). The fused products contained the kanamycin or spectinomycin resistance cassette, which was flanked by the downstream and upstream flanking regions of the target genes. In the second step of the LFH-PCR, the forward primer for the downstream flanking region and the reverse primer for the upstream flanking region were added to the LFH-PCR reaction to amplify the fused product. The LFH-PCR products were transformed into *B. subtilis* NCIB *comI*$^-$ (paragraph 2.6.7.) and similar to the first method, homologous recombination between the flanking regions of the target gene in the genome of *B. subtilis* NCIB *comI*$^-$ and in the LFH-PCR product exchanged the target gene with the resistance cassette. Transformants were positively selected by growth on LB agar with kanamycin or spectinomycin, respectively.

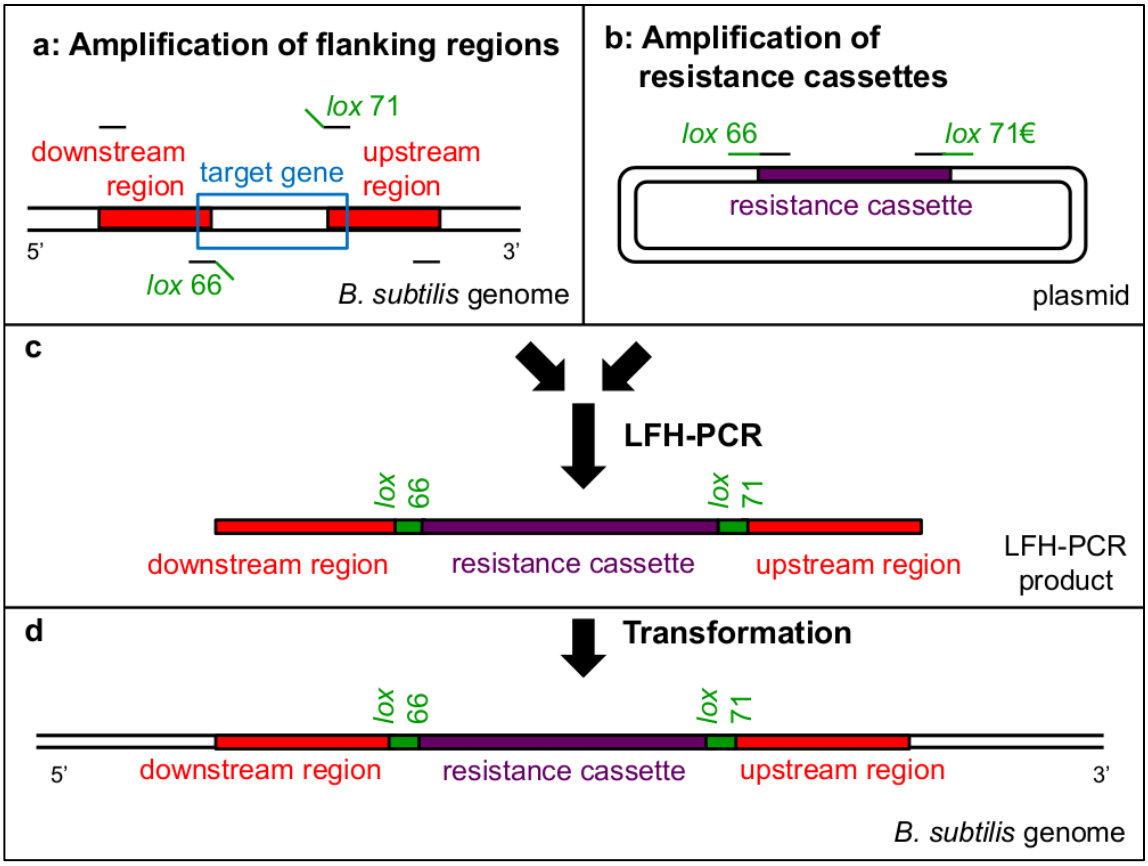

Figure 5: Overview of the Long Flanking Homology (LFH)-PCR for the gene deletion to generate amino acid auxotrophic *B. subtilis* strains (Yan et al., 2008). **a:** Flanking regions of the target gene in the *B. subtilis* genome (reading frame from 3' to 5') are amplified by PCR. **b**: Resistance cassettes for kanamycin or spectinomycin are amplified by PCR. **c:** The flanking regions of the target gene are fused with the resistance cassette with LFH-PCR. **d:** The LFH-PCR product is transformed into *B. subtilis* and the target gene is replaced by the resistance cassette by homologous recombination. Flanking regions of the target gene are marked in red, the target gene in marked in blue, the resistance cassette is marked in purple, and the *lox* sites are marked in green. Primers are indicated as black lines.

2.6.2. Design of the primers

Primers for the LFH-PCR were designed similar as described in paragraph 2.5.2. For that, primers were designed to amplify the downstream and upstream flanking regions of the target genes with a length of 500 bp to 700 bp (Table S5). Additional sequences were added to the 5' ends of those primers, which aligned within the target gene (Fig. 5). The additional sequences were the *lox* site 66 for the downstream flanking region and the *lox* site 71 for the upstream flanking region. The *lox* sites were added that way, that they had the same direction in the LFH-PCR product. Primers for the amplification of the kanymcin resistance cassette were oRGM7 and oRGM2. The spectinomycin resistance cassette was amplified with primers oRGM16 and oRGM17 (Table S6).

2.6.3. Amplification of the flanking regions of the target genes

At first, the target gene regions were amplified (table S7). Subsequently, the PCR products were used as template for the PCR to amplify the flanking regions of the target genes. It was not possible to do a colony PCR for the amplification of the flanking regions of the target genes, because the primers with the additional *lox* sites would have aligned to another sequence in the genome of *B. subtilis* NCIB *comI*$^{-}$.

For the generation of the template DNA, however, a colony PCR was performed. For that, the primers were used, which were designed for the first method, the gene deletion with deletion vectors (Table 8). The primers, which align outside of the flanking regions of the target genes, were used to amplify the target gene regions (i. e. primers with endings o_fw and o_rv). However, in the case of the *hisD* region, primers hisDd_fw and hisDu_rv had to be used to allow correct binding of the primers. For each gene region four reactions and one negative control were prepared as described in paragraph 2.5.11. However, there 2 µl Phusion High-Fidelity Polymerase was used. The colony PCR program differed such that the extension time was 90 s and the PCR contained 35 cycles. The four PCR products of one target gene region were pooled afterwards and analyzed in a 1 % agarose gel as described in paragraph 2.5.3. Subsequently, the PCR products were purified and DNA concentrations were measured as described in paragraph 2.5.7.

The purified PCR products were used as template for a PCR to amplify the flanking regions of the target genes with the Phusion High-Fidelity Polymerase (Table 15). Negative controls for the downstream flanking region of *lysA* and *pheA* and the upstream flanking region of *tyrA* were prepared without template DNA.

Table 15: Components of the PCR to amplify the flanking regions of the target genes for the LFH-PCR.

Compound	**Volume (µl)**
5 x Phusion High-Fidelity Buffer	10.0
dNTPs (10 mM)	1.0
Forward primer[1] (10 pmol μl^{-1})	2.5
Reverse primer[1] (10 pmol μl^{-1})	2.5
Template DNA	3.0 (about 10 ng)
Phusion High-Fidelity Polymerase	0.5
ddH2O	30.5

1: Primers are shown in table 8; primers with endings o_fw and o_rv used

The PCR program was designed as follows:

Initial denaturation:	98 °C for 30 s	
Denaturation:	98 °C for 10 s	
Annealing:	67.1 °C (1), 65.8 °C (2), 72 °C (3) for 20 s	} 35 x
Extension:	72 °C for 15 s	
Final extension:	72 °C for 7 min	
Holding:	10 °C∞	

Different annealing temperatures - (1) to (3) - were applied for the amplification of the flanking regions of the target genes:

(1) was used for the downstream flanking regions of *argH, hisD, lysA, tyrA, thrC,* and the upstream flanking region of *tyrA.*

(2) was used for the downstream flanking region of *trpC* and the upstream flanking regions of *argH, hisD, lysA,* and *trpC*.

(3) was used for the upstream flanking region of *thrC.*

Subsequently, the PCR products were analyzed in a 1 % agarose gel as described in paragraph 2.5.3. Then, the PCR products were purified and DNA concentrations were measured as described in paragraph 2.5.7.

2.6.4. Amplification of the resistance cassettes

The kanamycin resistance cassette was amplified using pTB120 *lox*-Neo-*lox* as template and oRGM2 and oRGM7 as primers (Table S7). Reactions for the amplification of the spectinomycin resistance cassette were prepared using pTB233 *lox*-Sp-*lox* as template and oRGM16 and oRGM17 as primers. Each PCR reaction was prepared as a 50 µl reaction with the Phusion High-Fidelity Polymerase (Table 16).

Table 16: Components of the PCR to amplify the resistance cassettes for the LFH-PCR.

Compound	Volume (µl)
5 x Phusion High-Fidelity Buffer	10.0
10 mM dNTPs	1.0
Forward primer[1] (10 pmol μl^{-1})	2.5
Reverse primer[1] (10 pmol μl^{-1})	2.5
Template (plasmidDNA)	0.5
Phusion High-Fidelity Polymerase	0.5
ddH2O	33.0

1: primers are shown in table S7

The PCR program was designed as follows:

Initial denaturation:	98 °C for 30 s	
Denaturation:	98 °C for 10 s	35 x
Annealing:	72 °C for 20 s	
Extension:	72 °C for 20 s	
Final extension:	72 °C for 7 min	
Holding:	10 °C ∞	

Finally, 10 µl PCR product was loaded onto a 1 % agarose gel and purified from the gel with the PureLink Quick Gel extraction and PCR purification Combo Kit, following the manufacturer's protocol. Bands were cut from the agarose gel and solubilized with Gel Solubilization Buffer. Furthermore, 1 gel volume isopropanol was added. Then DNA was purified and DNA concentrations were measured as described in paragraph 2.5.7.

2.6.5. Optimized ratio of resistance cassette to flanking regions in a LFH-PCR

A LFH-PCR was performed with the flanking regions of *argH* and the kanamycin resistance cassette with the Phusion High-Fidelity Polymerase (Table 17). For this, different ratios of resistance cassette to flanking regions were tested. Kanamycin resistance cassette and *argH* flanking regions were added in a ratio of 1.5 to 1, 1 to 1, 1 to 2 and 1 to 5. Negative controls with only flanking regions of *argH* in concentrations of 25 ng and 50 ng were prepared.

Table 17: Components of the LFH-PCR (part A).

Compound	**amount**
resistance cassette and amplified flanking regions of the target genes[1]	In a ratio of 1.5 to 1, 1 to 1, 1 to 2 and 1 to 5
5 x Phusion High-Fidelity Buffer	5.00 µl
dNTPs (Kapa Biosystems, Wilmington, USA)	0.50 µl
Phusion High-Fidelity Polymerase	0.25 µl
ddH_2O	to 25.00 µl

1: ratio of resistance cassette to each flanking region of the target genes in ng: 1.5 to 1 ratio: 37.5 ng to 25 ng; 1 to 1 ratio: 25 ng to 25 ng; 1 to 2 ratio: 25 ng to 50 ng; 1 to 5 ratio: 5 ng to 25 ng

The LFH-PCR program involved two parts. Part A involved the following steps:

Initial denaturation:	98 °C for 1 min	
Denaturation:	98 °C for 15 s	10 x
Annealing:	53 °C for 30 s	
Extension:	72 °C for 75 s	
Holding:	10 °C ∞	

Then, the forward primer for the downstream flanking region of *argH* and the reverse primer for the upstream flanking region were added to the reactions, each with a volume of 1.25 µl (10 pmol $µl^{-1}$; table S5). Part B of the LFH-PCR included the following steps:

Denaturation:	98 °C for 15 s	20 x
Annealing:	68 °C for 30 s	
Extension:	72 °C for 75 s + 5 s per cycle	
Final extension:	72 °C for 10 min	
Storage:	10 °C ∞	

Finally, 5 µl of the LFH-PCR products were analyzed in a 1 % agarose gel as described in paragraph 2.5.3.

2.6.6. LFH-PCR with all flanking regions

The test LFH-PCR showed that 1.5 to 1 ratio of resistance cassette to flanking regions was the best ratio. Therefore, LFH-PCR reactions were prepared with the kanamycin- and spectinomycin resistance cassettes and the flanking regions of the residual target genes with that ratio. The LFH-PCR was performed as described before in paragraph 2.6.5. Then, 5 µl of the LFH-PCR products was analyzed in a 1 % agarose gel as described in paragraph 2.5.3.

2.6.7. Transformation of LFH-PCR products into *B. subtilis*

Transformation with *B. subtilis* NCIB 3610 *comI*$^{-}$ was performed as described before in paragraph 2.5.15. For this, the complete LFH-PCR product was added to the transformation reaction. Furthermore, two negative controls without LFH-PCR product were prepared. The cultures were plated on LB agar with the respective amino acid (200 µM) and kanamycin (8 µg ml^{-1}) or spectinomycin (100 µg ml^{-1}). The negative controls were plated on LB agar with kanamycin (8 µg ml^{-1}) or spectinomycin (100 µg ml^{-1}). Pates were incubated at 37 °C for 3 d.

2.6.8. Colony PCR with transformants

A colony PCR was performed with the transformants as described before in paragraph 2.5.11. However, the extension time in the colony PCR program was prolonged to 2 min. PCR products were analyzed in an agarose gel as described in paragraph 2.5.3., however, a 0.8 % agarose gel was prepared, to allow better separation of the bands. Furthermore, the colonies were restreaked on LB agar with kanamycin (8 µg ml^{-1} and 5 µg ml^{-1}) and inoculated in 2 ml LB medium with kanamycin (8 µg ml^{-1}).

2.6.9. LFH-PCR with flanking regions of *argH* and *hisD*

The LFH-PCR was repeated with the aim to use only the correctly fused LFH-PCR product for transformation into *B. subtils* NCIB 3610 *comI*$^{-}$. For this, the flanking regions of *argH* and *hisD* were used because those LFH-PCR products showed the clearest bands in the gels in the previous experiments. LFH-PCR reactions were prepared as described before in paragraph 2.5.5. in a ratio of resistance cassette to flanking regions of 1.5 to 1. There, four to six replicates were prepared for each reaction. Then, 10 µl to 25 µl LFH-PCR product was loaded onto a 0.8 % agarose gel with six to eight lanes for each reaction.

The bands with the expected size of the LFH-PCR product were cut from the gel and the DNA was purified from the gel as described before in paragraph 2.6.4. Purification steps were altered to gain higher concentrations of DNA, because DNA purification from agarose gel with one band results in very low DNA concentrations. For purification, three to four bands of the same reaction were pooled on one Clean-up Spin Column in two replicates. Finally, the DNA of the two Columns was eluted into one reaction tube, where 10 µl or 15 µl autoclaved, double-distilled water was used for each elution step.

Transformation with the purified LFH-PCR products into *B. subtilis* NCIB 3610 *comI*$^{-}$ was performed as described in paragraph 2.5.15. and 2.6.7., respectively.

2.6.10. Colony PCR with transformants and digestion with *Kpn*I

A colony PCR with the transformants was performed as described before in paragraph 2.5.11. using an extension time of 2:50 min in the colony PCR program. The colony PCR products were digested with the FastDigest restriction enzyme *Kpn*I (Thermo Fisher Scientific). This enzyme cuts within the spectinomycin resistance cassette, but not within the region of *argH* or *hisD.* The reactions were prepared (Table S8) and incubated in a heating block at 37 °C for 45 min. Then, the restriction enzyme was inactivated by incubation at 80 °C for 5 min. Afterwards the digested colony PCR product (30 µl) was analyzed in an agarose gel as described in paragraph 2.5.3. However, a 0.8 % agarose gel was prepared.

2.6.11. Growth of transformants in minimal medium with and without amino acid

To verify, that the digestion of the colony PCR products of the transformants was unseccessful, the growth of the transformants in CSE minimal medium with and without amino acid was tested. For this, single colonies from the replica plates, which were prepared prior to the colony PCR were inoculated in 1 ml CSE medium with arginine or histidine (200 µM) and without amino acid. The cultures were incubated at 30 °C and for 24 h under shaking conditions (220 rpm). Then the OD (600 nm) was measured with the SpectraMax 190 microplate reader (Molecular Devices, Sunnyvale, USA). There 100 µl of the culture was analyzed in a 96 well plate. Blank reduction was performed with CSE medium.

After 24 h, the OD (600 nm) of the cultures was set to 0.1 and 10 µl of this dilution was used to inoculate 1 ml CSE medium with amino acid (200 µM) and without amino acid. These cultures were incubated at 30 °C for further 24 h under shaking conditions (220 rpm) and then the OD (600 nm) was measured again.

2.6.12. Sequencing of LFH-PCR products

LFH-PCR products with the flanking regions of *argH* and *lysA* and the kanamycin resistance cassette were sequenced. However, the primers, which were used in the LFH-PCR were incorrectly designed (Table S9): The *lox* sites were added to the 5' ends of the primers with incorrect orientation. Notably, the incorrect primers were not used for the previously described LFH-PCRs.

For purification, 25 µl LFH PCR product was loaded into a 1 % agarose gel as described in paragraph 2.5.3. Then the LFH-PCR products were purified from the gel as described previously in paragraph 2.5.7. and 2.6.4., respectively. The purified LFH-PCR product with the flanking regions of *argH* was sequenced with primers 1_LFH-d_fw and 1_LFH_u_rv (each 10 pmol μl^{-1}). Furthermore, the purified LFH-PCR product with the flanking regions of *lysA* was sequenced with primers 3_LFH-d_fw and 3_LFH_u_rv (each 10 pmol μl^{-1}). The sequencing results were analyzed using the webpage BLAST with *B. subtilis* 168 as reference genome (Altschul et al., 1990).

2.7. GFP- and mKATE-labeling of ordered *B. subtilis* strains

2.7.1. Verifying auxotrophy of ordered *B. subtilis* strains

This study was continued with *B. subtilis* strains, which were obtained from the *Bacillus* genetic stock center (Zeigler, 2000). Therefore, auxotrophy of these strains had to be verified first. Glycerol stocks of *B. subtilis* strains 1A208 (*hisH*), 1A62 (*trpA*), 1A543 (*trpC*), 1A553 (*trpA*) and 1A560 (*trpB*) were streaked on LB agar and incubated at 37 °C overnight. Single colonies were inoculated in 1 ml CSE medium with histidine and tryptophan, respectively (200 µM) and without amino acid and growth was observed as described previously in paragraph 2.6.11.

2.7.2. Transformation with phy-GFP and phy-mKATE

Plasmids phy-GFP and phy-mKATE were extracted from *E. coli* as described in paragraph 2.5.5. There, ampicillin (100 µg ml^{-1}) was used in the *E. coli* cultures, to select for the plasmids. Furthermore, concentrations of the plasmid DNA was measured as described in paragraph 2.5.5. Then the plasmids (1 µg) were transformed into the *B. subtilis* strains NCIB 3610 *comI*$^{-}$, 1A208 (*hisH*), 1A62 (*trpA*), 1A543 (*trpC*), 1A553 (*trpA*), and 1A560 (*trpB*) as described in paragraph 2.5.15. There, 200 mM of the amino acid, which the corresponding strain required for growth, was added to the cultures. The transformation cultures were plated on LB agar with chloramphenicol (5 µg ml^{-1}) and incubated at 37 °C for one day.

2.7.3. Starch hydrolysis test

Starch agar is a differential medium to analyze, whether an organism produces the extracellular enzymes α-amylase and Oligo-1,6-glucosidase, which hydrolyze starch (Leboffe and Pierce, 2010). The hydrolysis of starch is detected with Lugol solution, because iodine reacts with starch to form blue to black complexes (Lal and Cheeptham, 2015). After transformation with the plasmids phy-GFP and phy-mKATE, homologous recombination between sequences of the *amyE* gene in the plasmids and in the genome of *B. subtilis* strains should have occurred. There, the GFP or mKATE sequence was inserted into the *amyE* gene in the genome of the *B. subtilis* strains. Therefore, the *amyE* gene was disrupted so that the transformants could not degrade starch. To test whether the *amyE* gene was indeed disrupted, the transformants were streaked on starch agar. For that, four to eight transformants, which showed the brightest green or red color on the transformation plates, were used. After incubation at 37 °C for 44 h, the surface of the plates was flooded with Lugol solution. It was immediately documented, whether a halo was seen or not, where a halo indicated starch hydrolysis. Overnight cultures were prepared with the transformants, where the GFP or mKATE sequence was inserted into the *amyE* gene, and using 2 ml LB medium with chloramphenicol (5 µg ml^{-1}). The overnight cultures were incubated at 30 °C for 16 h under shaking conditions (220 rpm). Then, glycerol stocks were prepared as described in paragraph 2.3.

3. RESULTS

3.1 Determination of target genes

Target genes to generate *B. subtilis* strains that are auxotrophic for one amino acid were determined (table 18). The gene, which catalyzes the final step in the amino acid biosynthesis pathway, was considered as target gene. When it was not possible to generate auxotrophic strains by deleting the last gene in the biosynthetic pathway, the second last gene was chosen as the target gene. Those amino acids that can be biochemically converted into another amino acid were excluded from this study. This was the case for glycine and serine, which *B. subtilis* can biochemically convert into each other. Furthermore, those amino acids were excluded, which are synthesized via several pathways or which involve more than one enzyme in the final step in the pathway. This is true for alanine, asparagine, leucine, isoleucine, methionine, proline, aspartate, glutamine, and cysteine. Finally, valine was excluded, because many enzymes, which catalyze the formation of valine, are also required for the biosynthesis of isoleucine.

In case of arginine, histidine, lysine, and threonine the identified target genes in *B. subtilis* encode enzymes, which catalyze the final step in the amino acid biosynthesis pathway. However, for the generation of auxotrophic strains for tyrosine, phenylalanine and tryptophan the genes encoding the enzyme, which catalyzes the second last step in the amino acid biosynthesis pathway were targeted. In the case of tyrosine and phenylalanine three different gene products are involved in the final biosynthesis step. The last step in the biosynthesis of tryptophan requires the tryptophan synthase alpha chain and beta chain, which are encoded by two different genes.

Table 18: Identified target genes, whose deletion is predicted to result in the generation of amino acid auxotrophic *B. subtilis* strains. The respective gene product and the catalyzed reactions are presented.

Amino acid	Gene	Gene product	Catalyzed reaction
L-arginine	*argH*	argininosuccinate lyase	L-argino succinate to arginine
L-histidine	*hisD*	histidinol dehydrogenase	histidinal to L-histidine
L-lysine	*lysA*	diaminopimelate decarboxylase	meso-diaminopimelate to L-lysine
L-tyrosine	*tyrA*	prephenate dehydrogenase	prephenate to 4-hydroxyphenylpyruvate
L-phenylalanine	*pheA*	prephenate dehydratase	prephenate to phenylpyruvate
L-tryptophan	*trpC*	indole-3-glycerol phosphate synthase	1-(2-carboxyphenylamino)-1-deoxy-D-ribulose 5-phosphate to 1-C-(indol-3-yl) glycerol 3-phosphate
L-threonine	*thrC*	threonine synthase	O-phospho-L-homoserine to L-threonine

3.2. Gene deletion with a deletion vector

The first method to delete the target genes in *B. subtilis* involved the generation of a deletion vector. For this, the regions flanking the target genes in the *B. subtilis* genome were cloned into the MCSs of the plasmids pTB120 *lox*-Neo-*lox* and pTB233 *lox*-Sp-*lox.*

3.2.1. Amplification and digestion of the flanking regions of the target genes

The flanking regions of the target genes in *B. subtilis* were amplified by colony PCR. The PCR products showed one distinct band of expected size in the agarose gel (550 bp to 770 bp). No bands were seen in the negative controls. Subsequently, the resulting PCR products were double-digested. However, it was not possible to analyze in an agarose gel, whether the PCR products were completely digested. The difference in size between the undigested and digested PCR product was only two to six base pairs.

3.2.2. Extraction and digestion of plasmids

The plasmids pTB120 *lox*-Neo-*lox* and pTB233 *lox*-Sp-*lox* were extracted from *E. coli* and double-digested. Extracted plasmids had values of A260 nm to A280 nm ratio between 1.72 and 1.91 (Table 19). This value characterizes the purity of the DNA sample, where a value of two characterizes pure DNA (Glasel, 1995).

Undigested plasmids formed several bands in the agarose gel (Fig. 6a), which was most likely due to the different possible conformations of the plasmid. The upper band in the agarose gel represents a relaxed circle, which forms when a DNA strand is disrupted (Wink, 2006). In contrast, the lower band is highly supercoiled DNA. The intermediate bands represent the different topoisomers. Double-digested plasmids showed one distinct band of expected size (pTB120 *lox*-Neo-*lox*: 4,353 bp; pTB233 *lox*-Sp-*lox*: 4,022 bp, Fig. 6b). However, in the first and second attempt of generating deletion vectors, the plasmid pTB120 *lox*-Neo-*lox*, digested with *Hind*III and *Eco*RI formed two bands of unexpected size. One band had a size of approximately 3 kbp in the agarose gel, whereas the second band had a size of approximately 1.5 kbp (Fig. 6c). Furthermore, the plasmid pTB120 *lox*-Neo-*lox*, which was double-digested with *Sal*I and *Eco*RI did not form a band in the agarose gel.

After double-digestion, the PCR products and the plasmids were purified. The DNA samples with the digested and purified plasmids were less concentrated than the undigested plasmids (Table 19). Due to that decrease in concentrations during the purification, the PCR products were not purified prior to digestion. Furthermore, the concentrations and A260 nm to A280 nm ratios of the plasmids with the first insert were lower than of the plasmids without insert.

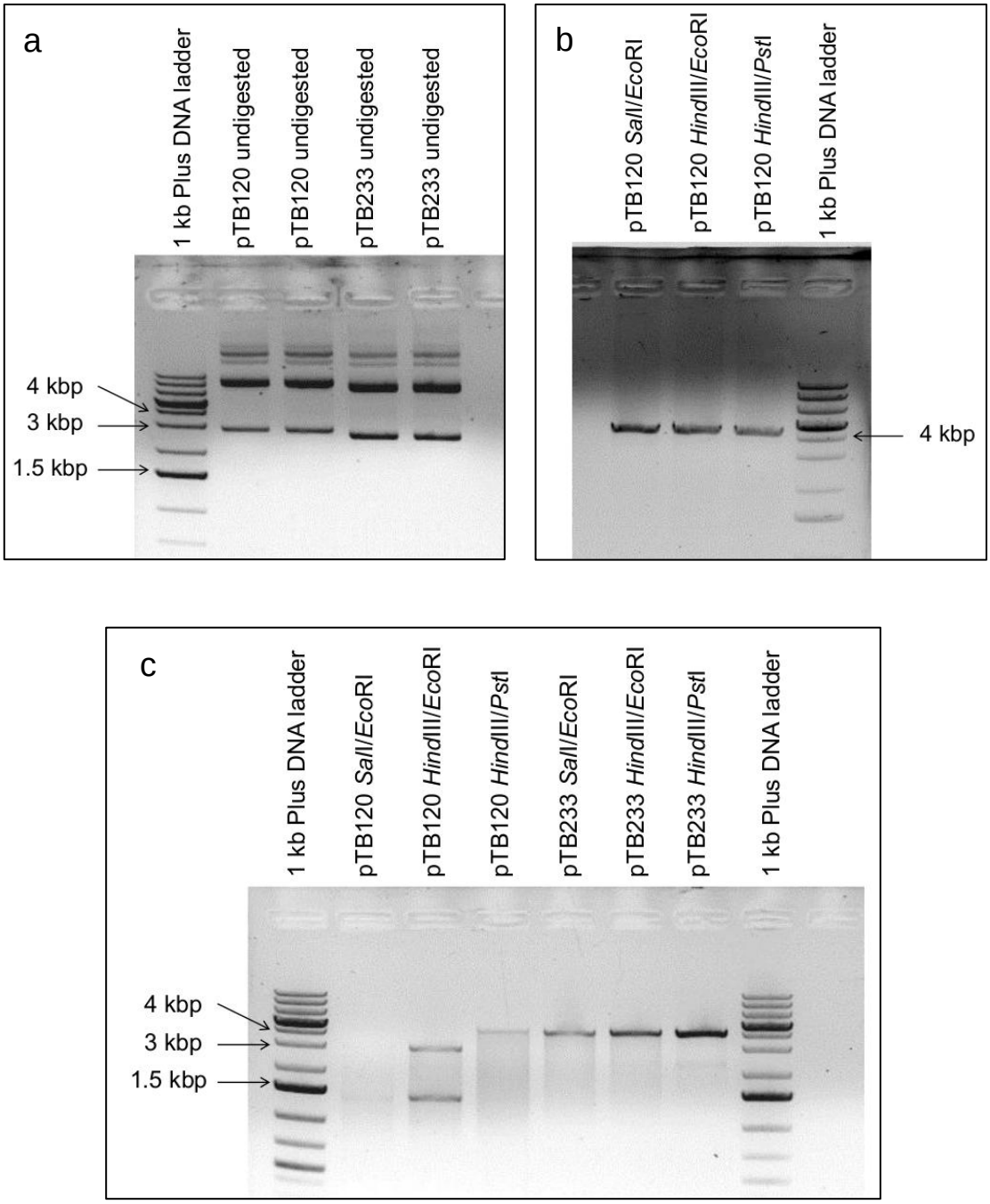

Figure 6: Agarose gels (1 %) with plasmids pTB120 *lox*-Neo-*lox* and pTB233 *lox*-Sp-*lox*, here abbreviated with pTB120 and pTB233. **a:** Undigested plasmids pTB120 and pTB233. **b:** Plasmid pTB120 double-digested with the given restriction enzymes. Bands are of expected size. **c:** Plasmids pTB120 and pTB233 double-digested with the given restriction enzymes. However, bands of pTB120 restricted with *Hind*III and *Eco*RI are of unexpected size.

Table 19: Concentrations of plasmids and PCR products for the gene deletion with a deletion vector. Single values of concentration were combined as a range of values.

	Concentration (ng μl^{-1})	A260 nm to A280 nm
Extracted plasmids	55 - 508	1.72 - 1.91
Double-digested and purified PCR products	10 - 28	1.57 - 1.86
Double-digested and purified plasmids	26 - 88	1.51 - 1.89
Double-digested and purified plasmids with 1st insert	12 - 18	1.69 - 1.80

3.2.3. Ligation and transformation into *E. coli*

The double-digested PCR products were ligated with the double-digested plasmids and transformed into *E. coli* for amplification. After three to four days, approximately 50 to 100 small colonies were observed on each transformation plate. Additionally, negative controls of the ligation reactions were prepared, using the double-digested plasmid but no PCR product, and transformed into *E. coli*. This enabled an estimation of self-cyclization of the plasmids despite treatment with SAP, which dephosphorylated the double-digested plasmids. When more colonies were on the plates with the potential transformants than with negative controls, the potential transformants were analyzed. This was true in most cases. However, several colonies grew on all transformation plates with the negative controls. Consequently, treatment with SAP did not prevent self-cyclization of all plasmids.

3.2.4. Analysis of potential transformants

A colony PCR was performed with the potential transformants to analyze whether the flanking regions of the target genes were cloned into the plasmids. The primers, which were used, could not align in the *E. coli* genome to produce a PCR product of 550 bp to 770 bp. Consequently, a PCR product of 550 bp to 770 bp showed that the flanking region of the target gene was cloned into the plasmids. In the agarose gels bands of expected size were seen for several PCR products (Table 20). This indicates that the flanking regions of the target gene were inserted into the plasmid in these potential transformants.

Table 20: Summary of the results of the colony PCR for the analysis of inserts in the plasmids pTB120 *lox*-Neo-*lox* and pTB233 *lox*-Sp-*lox*. The inserts are the downstream or upstream flanking regions of the presented target genes in *B. subtilis*. The results are sorted by the four attempts of generating deletion vectors.

	pTB120 *lox*-Neo-*lox*		**pTB233 *lox*-Sp-*lox***	
Attempt	**Downstream**	**Upstream**	**Downstream**	**Upstream**
1st	*pheA*[1], *trpC*[1]		*argH*, *tyrA*[1], *pheA*, *trpC*[1]	
2nd			*hisD*, *tyrA*, *pheA*, *trpC*, *thrC*	
3rd	*argH*[1], *hisD*, *lysA*[1], *tyrA*[1], *pheA*, *thrC*		*hisD*, *lysA*,	*tyrA*, *thrC*
4th	*argH*, *lysA*, *tyrA*[1], *thrC*[1]	*hisD, pheA, trpC*	*lysA*[1]	*hisD, pheA*[1], *trpC, thrC*

1: band with low intensity in the agarose gel

In those cases, where the PCR products formed bands of expected size in the agarose gels, plasmids where extracted from the respective potential transformants. Then the plasmids were digested with the same restriction enzymes, which were used for the plasmid digestion prior ligation. When the flanking regions of the target genes were cloned into the plasmids, the digested plasmids should form two distinct bands in an agarose gel: one band of the size of the plasmids (pTB120 *lox*-Neo-*lox*: 4,353 bp; pTB233 *lox*-Sp-*lox*: 4,022 bp) and one band of the size of the flanking regions of the target genes (550 bp to 770 bp). This was true for a few digested plasmids (Table 21). Notably, the digestion of the plasmids, which were extracted from potential transformants, lead to less positive results than the colony PCR with potential transformants.

Table 21: Summary of the analysis of the double-digested plasmids, which were extracted from potential transformants. It is presented for which flanking region of the target genes bands were seen in an agarose gel. The results are sorted by the four attempts of generating deletion vectors.

	pTB120 *lox*-Neo-*lox*		**pTB233 *lox*-Sp-*lox***	
Attempt	**Downstream**	**Upstream**	**Downstream**	**Upstream**
1st			*argH*	
2nd			*hisD*, *tyrA*, *pheA*, *thrC*	
3rd	*hisD*[1], *pheA*[1]			*tyrA*[1]
4th	*argH*, *lysA*	*trpC*		*hisD*, *trpC, thrC*

1: band with low intensity in the agarose gel

3.2.5. Transformation of the deletion vectors into *B. subtilis*

After the fourth attempt of generating deletion vectors, three deletion vectors had been created by cloning the downstream and upstream regions of the target genes into the plasmid pTB233 *lox*-Sp-*lox.* These were plasmids pTB233 *lox*-Sp-*lox* with inserted flanking regions of *hisD*, *tyrA*, and *thrC* and they were sequenced using primers T3 and T7 (electronic supplementary). Analysis of the sequencing results revealed that the flanking regions of *hisD*, *tyrA*, and *thrC* were correctly cloned into the plasmid pTB233 *lox*-Sp-*lox.* The plasmid pTB233 *lox*-Sp-*lox* with the inserted flanking regions of *tyrA* was falsely rejected. However, later analysis showed that also this plasmid was correctly cloned. The plasmids pTB233 *lox*-Sp-*lox* with the inserted flanking regions of *hisD* and *thrC* were transformed into *B. subtilis* NCIB 3610 *comI*$^{-}$. However, no transformants grew on the transformation plates after five days.

3.3. Gene deletion with LFH-PCR

3.3.1. Amplification of regions flanking the target genes and resistance cassettes

In the second gene deletion method the kanymcin and spectinimycin resistance cassettes were fused with the flanking regions of the target genes in *B. subtilis* with LFH-PCR. All amplified flanking regions of the target genes in *B. subtilis* formed distinct bands of expected size (570 bp to 790 bp) and a high intensity in the agarose gels. However, also the negative control PCR product of the downstream flanking region of *pheA*, which was prepared without template DNA, formed a distinct band of 600 bp. The other negative controls formed no bands in the agarose gels. This indicates contamination of the primers 3_LFH_d_fw and 3_LFH_d_rv, which were used for the amplification of the downstream flanking region of *pheA*. Afterwards, the PCR products were purified and the concentrations of the purified PCR products were measured (Table 22). Notably, the amplified upstream flanking region of *trpC* had a divergent low concentration (16.55 ng μl^{-1}).

The kanamycin and spectinomycin resistance cassettes were amplified by PCR with the plasmids pTB120 *lox*-Neo-*lox* and pTB233 *lox*-Sp-*lox* as template. All PCR products formed three distinct bands in the agarose gels and no negative control formed a band. The bands with the expected size (pTB120 *lox*-Neo-*lox*: 1,390 bp; pTB233 *lox*-Sp-*lox*: 1,060 bp) were cut from the gel and purified. However, the concentrations of the purified resistance cassettes were low (Table 22).

Table 22: Concentrations of purified PCR products and kanamycin and spectinomycin resistance cassettes for the LFH-PCR. Single concentrations of 14 PCR products were combined as a range of values. Furthermore, the two resistance cassttes with three replactes each, were combined as a range of values.

	Concentration (ng μl^{-1})	**A260 nm to A280 nm**
Purified PCR products	32 - 136[1]	1.79 – 1.96
Purified resistance cassettes	9 - 70	1.78 - 1.96

1: Concentration of the amplified upstream flanking region of *trpC* is not included (16.55 ng μl^{-1})

3.3.2. LFH-PCR

The purified flanking regions of the target genes were fused with the purified resistance cassettes in a LFH-PCR. For this, the optimal ratio of resistance cassettes to flanking regions was analyzed. At first different ratios were tested with the kanamycin resistance cassette and the amplified downstream and upstream flanking regions of *argH* in a LFH-PCR (1.5 to 1, 1 to 1, 1 to 2, and 1 to 5). The LFH-PCR product with the ratio of 1.5 to 1 formed the band with the highest intensity with the expected size in the agarose gel (expeted size 2.8 kbp; Fig. 7). However, this band was also formed by the negative controls, which were prepared with the flanking regions without the resistance cassette. Nevertheless, this band was less bright than the LFH-PCR product with the ratio of resistance cassette to flanking regions of 1.5 to 1. Notably, all LFH-PCR products formed several bands in the agarose gel.

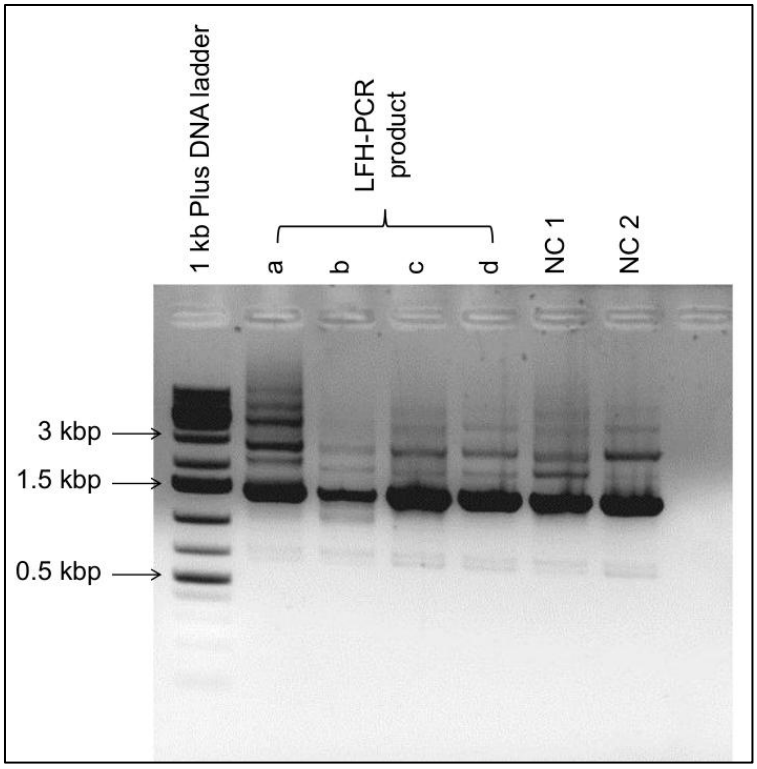

Figure 7: Agarose gel (1 %) with the LFH-PCR products with the kanamycin resistance cassette and the flanking regions of *argH.* Different ratios of resistance cassette to flanking regions were tested. a: ratio of 1.5 to1; b: ratio of 1 to 1; c: ratio of 1 to 2; d: ratio of 1 to 5. Two negative controls were prepared: NC 1 with 25 ng of each amplified flanking region of *argH* and NC 2 with 50 ng of each amplified flanking region of *argH.*

LFH-PCR was performed with all amplified flanking regions and both resistance cassettes with the ratio of resistance cassette to flanking regions of 1.5 to 1. All LFH-PCR products formed several bands in the agarose gels and the bands of the expected size were not the brightest bands. The theoretical size of the LFH-PCR products with the kanamycin resistance cassette was 2.74 kbp to 2.85 kbp and with the spectinomycin resistance cassette 2.4 kbp to 2.54 kbp. Overall, the LFH-PCR products with the kanamycin resistance cassette formed brighter bands of the expected size than the LFH-PCR products with the spectinomycin resistance cassette. The LFH-PCR product with the kanamycin resistance cassette and the flanking regions of *trpC* formed a band of expected size of low intensity in the agarose gel. Furthermore, the bands of expected size of the LFH-PCR products with the spectinomycin resistance cassette and the flanking regions of *tyrA, pheA, trpC,* and *thrC* were of low intensity.

3.3.3. Transformation of LFH-PCR products into *B. subtilis*

Although several LFH-PCR products formed bands of the expected size of low intensity in the agarose gels, all LFH-PCR products were used for transformation into *B. subtilis* NCIB *comI*$^-$. After three days, several colonies were observed on the transformation plates (Table 23). However, potential transformants were obtained only with the LFH-PCR products of the flanking regions of *tyrA, trpC*, and *thrC*. Notably, these LFH-PCR products formed bands of the expected size of low intensity in the agarose gel before. Furthermore, in case of the potential transformants with the LFH-PCR product with the kanamycin resistance cassette and the flanking regions of *trpC*, almost as many colonies were observed with the negative control than with the LFH-PCR products.

Table 23: Colonies on the transformation plates with the LFH-PCR products with the kanamycin and spectinomycin resistance cassette and the flanking regions of the presented genes.

Gene	Kanamycin resistance cassette		Spectinomycin resistance cassette	
	LFH-PCR	**Negative control**	**LFH-PCR**	**Negative control**
tyrA	33 colonies	4 colonies	1 colony	0 colonies
trpC	20 colonies	18 colonies		
thrC	12 colonies	0 colonies		

3.3.4. Analysis of the potential transformants

A colony PCR was performed with the potential transformants and the PCR products were analyzed in a 0.8 % agarose gel (Fig. 8). If the resistance cassette has been correctly inserted into the genome of *B. subtilis*, the PCR product of the transformant should be bigger than the PCR product of *B. subtilis* without inserted resistance cassette (Table 24).

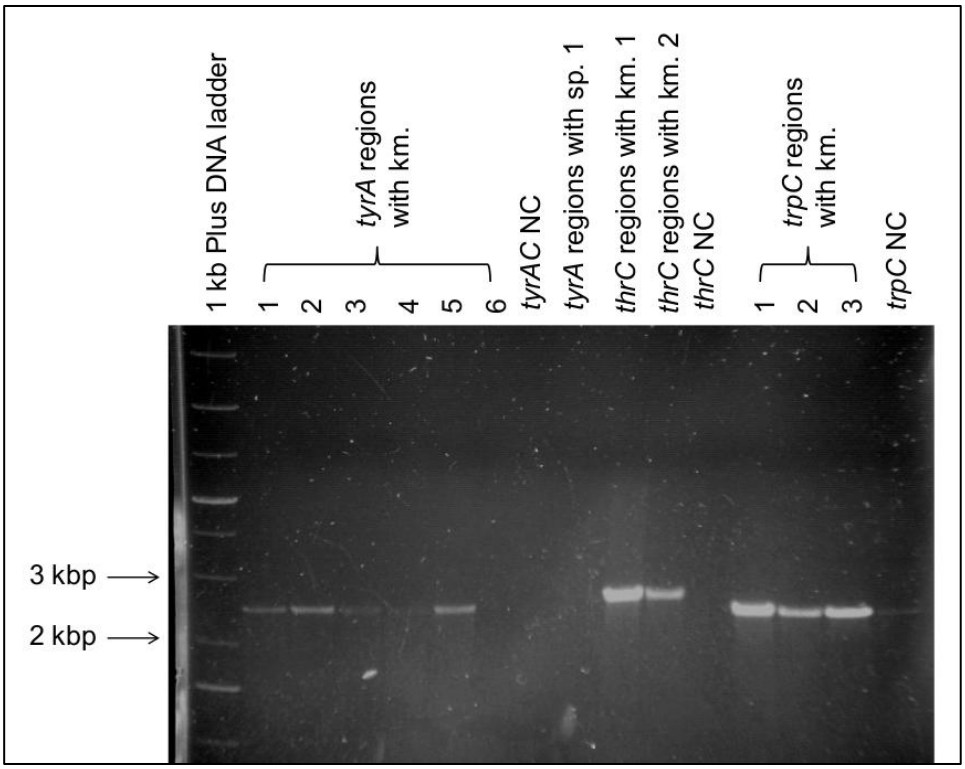

Figure 8: Agarose gel (0.8 %) with colony PCR products for the analysis of potential transformants with LFH-PCR products. Analyzed potential transformants were numbered. km: kanamycin resistance cassette. sp: spectinomycin resistance cassette. NC: Negative control, which was the LFH-PCR product without resistance cassette.

Table 24: Expected size of the amplified gene regions and the gene regions with inserted kanamycin resistance cassette after colony PCR of potential transformants.

Gene	Gene region	Gene region with inserted kanamycin resistance cassette
tyrA	2.46 kbp	2.49 kbp
trpC	2.28 kbp	3.07 kbp
thrC	2.46 kbp	3.05 kbp

The PCR product of the potential transformant containing the spectinomycin resistance cassette and the flanking regions of *tyrA* did not form a band in the agarose gel. Furthermore, no difference in size between the band of the potential transformant of *tyrA* with the kanamycin resistance cassette and the control was seen, which was the amplified *tyrA* gene region of *B. subtilis*. The band for the potential transformants of *trpC* should be 807 bp larger than the negative control, but no difference in size was detected. Consequently, the *trpC* gene of *B. subtilis* was not exchanged by the kanamycin resistance cassette in the analyzed colonies. Since almost as many colonies were on the transformation plates with the LFH-PCR products with the *trpC* flanking regions than on the control plates, no potential transformants of *trpC* were analyzed further.

In case of the successful transformant of *thrC*, the PCR product should have formed a band with a size of 3,068 bp. However, the band appeared to be slightly smaller, but the size could not be exactly determined. Furthermore, the control for *thrC* did not form a band in the agarose gel. Colony PCR was repeated with the residual transformants of *thrC*. The PCR products formed bands of high intensity of the same size as the control, which was the amplified *thrC* gene region.

Since it was not possible to draw exact conclusions from the agarose gel with the PCR products, the potential transformants of *tyrA* and *thrC* were inoculated in LB medium with kanamycin (5 µg ml^{-1} and 8 µg ml^{-1}) and tyrosine and threonine, respectively (200 µM). However, no growth was observed with either kanamycin concentration. Accordingly, the genes *tyrA* and *thrC* have not been replaced by the kanamycin resistance cassette.

3.3.5. Repeated LFH-PCR with flanking regions of *argH* and *hisD*

Since the transformation with the whole LFH-PCR products was not successful, the process was repeated. However, only the LFH-PCR products of expected size were used for transformation. LFH-PCR was performed with the flanking regions of *argH* and *hisD*, because previous LFH-PCR products of those formed the brightest distinct band of expected size in the agarose gels. The band of expected size in the agarose gel, which was formed by the LFH-PCR product with the flanking regions of *argH* and *hisD*, was cut from the gel and purified. However, the bands in the agarose gel were of low intensity. The purified LFH-PCR products had concentrations of 2 ng μl^{-1} to 11 ng μl^{-1} and values of A260 nm to A280 nm ratio of 1.52 to 1.90.

3.3.6 Transformation of the purified LFH-PCR products into *B. subtilis*

The whole purified LFH-PCR products were used for transformation with *B. subtilis* NCIB 3610 *comI*$^{-}$, which equals concentrations of 25 ng to 113 ng. After four days, several colonies had grown on the transformation plates: In case of potential transformants with LFH-PCR products, which contained flanking regions of *argH* and the spectinomycin resistance cassette, two colonies grew. However, also two colonies grew on the plate with the negative control, which was obtained from LFH-PCR products without the resistance cassette.

On the plate with the potential transformants with LFHP-PCR products of flanking regions of *hisD* and the spectinomycin resistance cassette, one colony grew. Notably, also three colonies were observed on the transformation plate with the negative control. No colonies were observed on the transformation plates with the cultures, which were transformed with LFH-PCR products containing the kanamycin resistance cassette.

3.3.7. Analysis of the potential transformants of *argH* and *hisD*

Although colonies were observed on the plates with the negative controls, the colonies of the transformation plates were analyzed. For this, a PCR was performed with the potential transformants, where the *argH* and *hisD* regions were amplified. Afterwards, the PCR products were digested with *Kpn*I. This enzyme cuts within the spectinomycin resistance cassette but not within the regions of *argH* or *hisD.* Therefore, in case of successful insertion of the spectinomycin resistance cassette into the genome of *B. subtilis*, two bands were expected to be seen in the agarose gel. However, when the digested PCR products were analyzed, only bands of the size of the amplified gene regions were visible.

To verify that the target genes in *B. subtilis* were not replaced by the spectinomycin resistance cassette, the colonies of the transformation plates for *argH* and *hisD* were grown in minimal CSE medium with and without arginine or histidine. If the *argH* and *hisD* genes had been exchanged with the spectinomycin resistance cassette, the colonies would have been expected to grow to low OD (600 nm) values. However, the cultures without amino acid grew to OD (600 nm) values of 0.25 to 1.2. Accordingly, the colonies on the transformation plates were not auxotrophic for arginine or histidine.

3.3.8. Sequencing of LFH-PCR products

The LFH-PCR products with the flanking regions of *argH* and *lysA* and the kanamycin resistance cassette, which were produced with incorrect primers, were sequenced (electronic supplementary). There, the *lox* sites were added to the 5’ ends of the primers with incorrect orientation. Notably, the incorrect primers were not used in the previously described LFH-PCRs. Analysis of the sequences showed, that the flanking regions of *argH* and *lysA* did not fuse with the kanamycin resistance cassette during the LFH-PCR. Instead, the amplified flanking regions fused with the homologous amplified flanking region.

3.4. GFP- and mKATE-labeling of ordered *B. subtilis* strains

3.4.1 Verifying auxotrophy of ordered *B. subtilis* strains

The ordered *B. subtilis* strains were grown in CSE minimal medium with and without histidine or tryptophan to verify their auxotrophy. The strains, which were incubated without amino acid grew distinctly less than the strains, which were incubated with amino acid (Fig. 9). Therefore, the strains are auxotrophic for histidine and tryptophan, respectively.

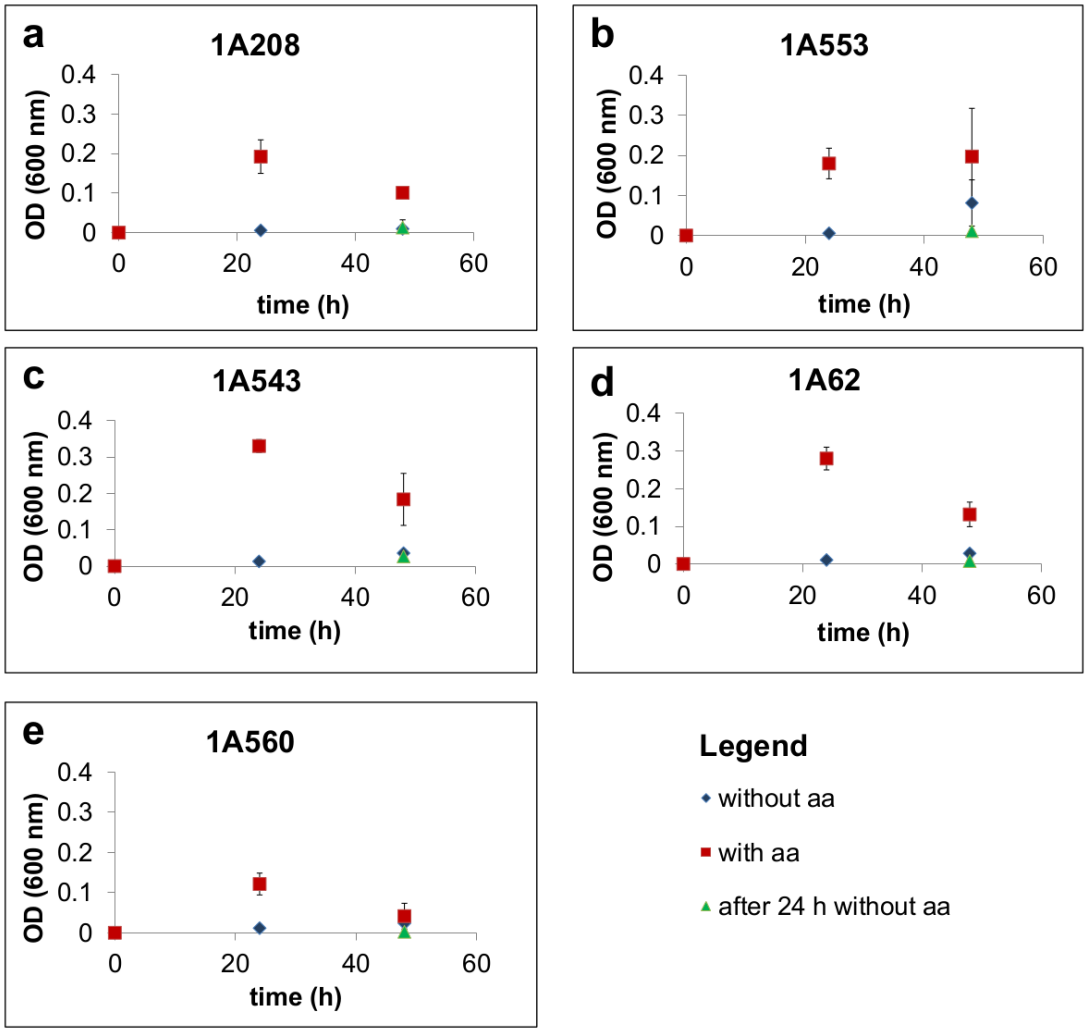

Figure 9: Growth of ordered *B. subtilis* strains in minimal medium with and without amino acid. After 24 h, the cultures, which were previously grown with amino acid, where inoculated into minimal medium without amino acid (Indicated by green triangle). **a:** Growth of *B. subtilis* 1A208. **b:** Growth of *B. subtilis* 1A553. **c:** Growth of *B. subtilis* 1A543. **d:** Growth of *B. subtilis* 1A62. **e:** Growth of *B. subtilis* 1A560.

3.4.2. GFP- and mKATE-labeling

The ordered auxotrophic *B. subtilis* strains and *B. subtilis* NCIB *comI*$^-$ were labeled with the two fluorescent proteins GFP and mKATE. One day after transformation, approximately 100 colonies with green or red color had grown per plate. However, the colonies had different color intensities. No transformants were obtained with *B. subtilis* 1A560, which is auxotrophic for tryptophan.

The transformants with the brightest color were analyzed with a starch hydrolysis test. When the GFP and mKATE sequence was inserted into the *B. subtilis* genome, the *amyE* gene was disrupted. Therefore, successfully transformed *B. subtilis* strains were not able to hydrolyze starch. Iodine reacts with starch and blue to black complexes are formed (Lal and Cheeptham, 2015). Accordingly, no halo should be seen on the starch agar plates with the transformants after addition of Lugol solution. This was true for one to two analyzed transformants of each transformation plate, except for *B. subtilis* 1A560, where transformation was unsuccessful. Accordingly, GFP- and mKATE-labeled *B. subtilis* strains NCIB 3610 *comI*$^-$, 1A208, 1A553, 1A543, and 1A62 were obtained.

4. DISCUSSION

The objective of this thesis was to analyze the characteristics of nanotube formation in *B. subtilis*. For this, cocultures should be analyzed composed of amino acid overproducing *E. coli* cells and *B. subtilis* cells, which are auxotrophic for the corresponding amino acid. The required amino acid auxotrophic *B. subtilis* strains should be generated in this thesis. At first, several genes were identified, where gene deletion potentially results in amino acid auxotrophy.

4.1. Determination of target genes

For the generation of amino acid auxotrophic *B. subtilis* strains, seven different target genes were identified. The list of genes included *argH*, *hisD*, *lysA*, *tyrA*, *pheA*, *trpC*, and *thrC*, which were the same genes as were deleted to generate auxotrophic *E. coli* strains by Bertels et al. (2012). Similarities and differences in the identification of target genes to be deleted for the generation of auxotrophic *E. coli* and *B. subtilis* strains are presented in table 25.

Notably, the biosynthesis pathways of phenylalanine and tyrosine are intimately connected in *B. subtilis* (BsubCyc database (Caspi et al., 2014)). Therefore, the generation of a phenylalanine auxotrophic strain can result in a strain, which is auxotrophic for phenylalanine and tyrosine and *vice versa*. However, the determined target genes *pheA* and *tyrA* are specific for each biosynthesis pathway and are not involved in the biosynthesis of the respective other amino acid.

To generate *B. subtilis* strains auxotrophic for threonine, *thrC* was chosen as target gene. However, threonine can additionally be synthesized by the reaction from L-2-aminoacetoacetate to threonine, which is catalyzed by the gene product of *tdh*. This is also true for *E. coli*, but nevertheless, the deletion of *thrC* resulted in a threonine auxotrophic strain in the study of Bertels et al. (2012). Therefore, the target gene *thrC* was not excluded in this thesis.

The genes *hisD* and *trpC*, which have been identified as possible target genes to generate *B. subtilis* strains auxotrophic for histidine and tryptophan, were the same genes, as were deleted or mutated in the ordered *B. subtilis* strains.

The ordered *B. strains*, which were *hisD*$^-$ and *trpC*$^-$, were auxotrophic for histidine and tryptophan. Therefore, the gene deletion of *hisD* and *trpC* with a deletion vector or with a LFH-PCR product should have resulted in strains auxotrophic for histidine and tryptophan, respectively.

Different from the design for auxotrophic *E. coli* strains (Bertels et al., 2012), the chosen target genes for *E. coli* auxotrophs of isoleucine, leucine, methionine, and proline were not considered as target genes in this thesis. Bertels et al. (2012) chose *ilvA* as target gene for isoleucine auxotrophs. This gene encodes the enzyme threonine dehydratase, which catalyzes the reaction from threonine to 2-oxobutanoate. However, this is the sixth last step in the biosynthesis pathway of isoleucine in *B. subtilis*. Therefore, *ilvA* was not considered as target gene in this study, because too many other reactions would be affected by deletion of that gene.

The gene *leuB* was considered as target gene for generating *E. coli* cells auxotrophic for leucine by Bertels et al. (2012). This gene encodes the 3-isopropylmalate dehydrogenase, which catalyzes the reaction from 3-isopropylmalate to 2-isopropyl-3-oxosuccinate. This reaction is the third last step in the biosynthesis of leucine in *B. subtilis*. However, the enzyme also catalyzes the reaction from D-erythro-3-methylmalate to 2-oxobutanoate. Since this enzyme is involved in 2-oxocarboxylic acid metabolism, C5-Branched dibasic acid metabolism, and valine, leucine, and isoleucine biosynthesis in *B. subtilis*, *leuB* was also not considered as target gene in this thesis.

For *E. coli* auxotrophs of methionine, the gene *metB* was considered as target gene (Bertels et al., 2012). Without the gene product of *metB,* the biosynthesis of cystathionine is not possible, which is the precursor for methionine. In *B. subtilis* the respective gene catalyzing this reaction is *yicI*. However, deletion of that gene would not generate an auxotroph for methionine. This is because cystathionine can be synthezised with the gene product of *yrhB*, which is absent in *E. coli*.

In *E. coli* the target gene for generating auxotrophs for proline is *proC*. Its gene product is the pyrroline-5-carboxylate reductase, which catalyzes the reaction from 1-pyrroline-5-carboxylate to L-proline. In *B. subtilis,* three isoenzymes catalyze this last step in the biosynthesis of proline. These enzymes are the gene products of the genes *proG*, *proH,* and *proI*. Therefore, all three genes would have to be deleted.

Deletion of one gene, which encodes enzymes catalyzing earlier steps in the biosynthesis of proline, is not possible. Precursors of proline can be synthesized in several different pathways.

Table 25: Similarities and differences in the identification of target genes to be deleted for the generation of auxotrophic *E. coli* (Bertels et al., 2012) and *B. subtilis* strains (this study).

Amino acid	**Target gene in Bertels et al., (2012)**	**Target gene in this study**
L-asparagine	excluded	excluded
L-aspartate	excluded	excluded
L-threonine	*thrC*	*thrC*
L-methionine	*metB*	excluded
L-lysine	*lysA*	*lysA*
L-isoleucine	*ilvA*	excluded
L-alanine	excluded	excluded
L-leucine	*leuB*	excluded
L-valine	excluded	excluded
L-proline	*proC*	excluded
L-glutamate	excluded	excluded
L-glutamine	excluded	excluded
L-histidine	*hisC*	*hisC*
L-arginine	*argH*	*argH*
L-cysteine	excluded	excluded
L-serine	excluded	excluded
L-glycine	excluded	excluded
L-tryptophan	*trpC*	*trpC*
L-tyrosine	*tyrA*	*tyrA*
L-phenylalanine	*pheA*	*pheA*

4.2. Generation of deletion vectors

Two different methods were applied to delete the identified genes in *B. subtilis*: deletion vectors were generated and LFH-PCR was performed. The generation of deletion vectors however, was successful only in the case of the plasmid pTB233 *lox*-Sp-*lox* into which the flanking regions of of *hisD*, *tyrA*, and *thrC* were cloned. In many cases, the cloning of the flanking regions of the target genes into the plasmid was inefficient, because several approaches were necessary for cloning one flanking region into the plasmid. A possible problem could have been the double-digestion of the amplified flanking regions of the target genes. They could not be analyzed in the agarose gels, because of the small difference in size between undigested and digested PCR product. However, by analysis of the double-digested plasmids in agarose gels, it was verified, that the double-digestion of the plasmids pTB120 *lox*-Neo-*lox* and pTB233 *lox*-Sp-*lox* was successful. Thus, the restriction enzymes, which were used, were active. The amplified flanking regions of the target genes were double-digested at the ends and therefore, the double-digestion might have been incomplete. However, additional base pairs were added to the 5' ends of the primers for the amplification of the flanking regions of the target genes to ensure complete double-digestion, as recommended by New England BioLabs (Cleavage Close to the End of DNA Fragments, 2015).

The amplified flanking regions of the target genes were not purified prior double-digestion, because of the loss of concentration during the purification process. Therefore, the PCR buffer might have interfered with the restriction enzymes. However, the polymerase could not extend the double-digested PCR products, because the polymerase has an extension temperature of 72 °C, whereas the double-digestion reactions were incubated at 37 °C.

Furthermore, in attempt one and two of generating deletion vectors, the plasmid pTB120 *lox*-Neo-*lox*, which was digested with *Hind*III and *Eco*RI unexpectedly formed two bands in the agarose gel. This indicates that the plasmid was cut at a second position due to star activity of the restriction enzymes or due to mechanical force. Therefore, the downstream flanking regions of the target genes could not be cloned into the plasmid pTB120 *lox*-Neo-*lox*, which was digested with *Hind*III and *Eco*RI.

4.3. LFH-PCR

Transforming *B. subtilis* with LFH-PCR products did not result in auxotrophic *B. subtilis* cells. The amplified resistance cassettes, which should be fused with the flanking regions of the target genes in the LFH-PCR had low concentrations. This was most likely due to the purification from agarose gels.

LFH-PCR products formed several bands besides the bands of expected size in the agarose gels. The LFH-PCR products, which were produced with incorrect primers, where the *lox* sites were added in incorrect orientation, were sequenced. According to the analysis of these sequencing results, the amplified flanking regions of the target genes fused with each other. When the downstream and upstream flanking regions of a target gene fuse due to the very similar *lox*-sites at their ends, these products can also be amplified in the LFH-PCR. This is, because the forward primer for the downstream flanking region of the target genes and the reverse primer for the upstream flanking region were used in the LFH-PCR. Four fused flanking regions of the target genes can form a product of similar size as the intended fusion product of downstream and upstream flanking regions of the target genes and the resistance cassette.

Although the sequencing results were obtained with incorrect primers, it has to be assumed, that the flanking regions of the target genes, which were amplified with correct primers, could have fused due to the similar *lox*-sites at their ends. Furthermore, the resistance cassettes might have fused in the LFH-PCR. However, these fusion products would not have been amplified with the primers used in the LFH-PCR. Consequently, the sequencing results suggest that there was competition between unintended fusion of DNA molecules and the intended fusion of flanking regions of the target genes and the resistance cassette in the LFH-PCR. Therefore, the desired fusion product was formed in too low amounts for successful transformation. The concentrations of the fusion products of downstream and upstream flanking regions of the target genes and the resistance cassettes could not be increased by purification of the LFH-PCR products from the agarose gel. Purified LFH-PCR products had concentrations of 2 ng μl^{-1} – 11 ng μl^{-1}, whereas the transformation protocol suggested utilization of 1 µg DNA (iGEM Groningen, 2015).

4.4. Transformation

When the deletion vectors were transformed into *B. subtilis*, no transformants were obtained, although the recommended concentration of 1 µg plasmid DNA was used for transformation (iGEM Groningen, 2015). However, frequencies of transformation are usually very low; they range between 0.1 % and 1.0 % (Madigan et al., 2010). Furthermore, only 10 % to 20 % of a *B. subtilis* population are naturally competent, which means that they are able to be transformed (Hamoen et al., 2003). Nevertheless, low abundant transformants can be selected for with selection markers as antibiotic resistances (Madigan et al., 2010). Possibly, the *B. subtilis* cells were transformed with the deletion vector, but that transformation was lethal for the cells due to interference with flanking genes of the target genes. However, the flanking genes of *hisD* and *thrC* are not essential genes (SubtiWiki, 2016; a; b).

Furthermore, transformation with LFH-PCR products into *B. subtilis* did not result in auxotrophic strains. For reasons described earlier, the LFH-PCR products had very low concentrations (2 ng μl^{-1} – 11 ng μl^{-1}), which was below the recommended transformation DNA concentration of 1 µg (iGEM Groningen, 2015). However, the minimum concentration of DNA, which results in discernible transformants, is 0.01 ng μl^{-1} (Madigan et al., 2010). When transformation was performed with LFH-PCR products, the transforming DNA likely included a mixture of intended fusion products of flanking regions of the target genes and the resistance cassette and unintended fusion products. This possibly decreased the likelihood of yielding intended transformants.

4.5. Kanamycin and spectinomycin as selection markers

Potential transformants were selected with kanamycin or spectinomycin. However, several *B. subtilis* colonies, which were identified as kanamycin sensitive subsequently, did grow on LB agar supplemented with kanamycin. Due to earlier observations, *B. subtilis* NCIB 3610 *comI*$^{-}$ sometimes grows with 5 µg ml^{-1} kanamycin, whereas it sometimes is sensitive to such a concentration of kanamycin (Gallegos-Monterrosa, 2015). However, *B. subtilis* NCIB 3610 *comI*$^{-}$ did not grow with 8 µg ml^{-1} kanamycin, when the kanamycin resistance was tested for this study. Therefore, potential transformants were always selected with 8 µg ml^{-1} kanamycin.

Growth of sensitive *B. subtilis* NCIB 3610 *comI*$^{-}$ colonies, despite kanamycin concentrations of 8 µg ml^{-1}, could be explained with the process of preparing the media: 12.8 µl of a kanamycin stock solution (50 mg ml^{-1}) was added to 80 ml LB agar. Despite subsequent mixing of the medium, the small volume of kanamycin solution might not have been equally distributed in the LB agar. This would have allowed sensitive cells to grow. Due to the manufacturer's information, kanamycin does not degrade during incubation at 37 °C for four days (Safety data sheet. Kanamycin sulfate, 2015).

Less frequently than with kanamycin, sensitive *B. subtilis* NCIB 3610 *comI*$^{-}$ colonies grew on LB agar with spectinomycin (100 µg ml^{-1}). For supplementation with spectinomycin, 800 µl of a spectinomycin stock solution (10 mg ml^{-1}) was added to 80 ml LB agar. This volume of 800 µl was easier to blend in the medium. Growth of sensitive colonies on LB agar with spectinomycin might be due to long storage and multiple thawing of the spectinomycin stock solution. This might have led to partial degradation of the spectinomycin stock solution.

4.6. Analysis of potential transformants

When potential transformants of *E. coli* with the deletion vectors were analyzed, colony PCR lead to more positive results than the digestion of the plasmids, which were extracted from the potential transformants. Either the colony PCR gave false positive results, or the digestion of the extracted plasmids was unsuccessful and cloned plasmids were incorrectly rejected. However, primers used to amplify the flanking regions of the target genes did not bind within the genome of *E. coli* or within the plasmids pTB120 *lox*-Neo-*lox* and pTB233 *lox*-Sp-*lox* to produce PCR products of 550 bp to 770 bp. Thus, only if the amplified flanking regions of the target genes have been cloned into the plasmids pTB120 *lox*-Neo-*lox* and pTB233 *lox*-Sp-*lox*, colony PCR should have resulted in products of 550 bp to 770 bp.

Potential transformants with LFH-PCR products were analyzed with colony PCR. However, it was difficult to exactly determine the size of the bands in the agarose gels. Digestion of the amplified gene regions of the potential transformants was more exact than analyzing the colony PCR products in agarose gels. Growth of the potential transformants in minimal medium without supplemented amino acid suggested, that transformation with LFH-PCR products was unsuccessful.

4.7. Alternative methods for gene deletion in *B. subtilis*

Since no auxotrophic *B. subtilis* strains were obtained with the generated deletion vectors and LFH-PCR products, alternative gene deletion methods were researched. Suicide vectors are not recommended for introducing gene deletions in *B. subtilis* because the existent systems have not been proven effective and suitable vectors for *B. subtilis* are lacking (Wenzel and Altenbuchner, 2015). Furthermore, gene deletion systems, which involve toxic molecules, are disadvantageous because there development of unintended suppressor mutations is likely.

Wenzel and Altenbuchner (2015) described a new, markerless method of gene deletion in *B. subtilis*. The foundation of the method is that strains, which harbor the *manP* gene but are mutants of the mannose-6-phosphate dehydrogenase (*manA*), are sensitive to the presence of mannose (Wenzel et al., 2011). In contrast, strains where both genes *manP* and *manA* are present, are resistant to mannose. This method requires a *B. subtilis* strain, where the *manP* and *manA* genes were deleted. Then a vector needs to be developed, which encodes the *manP* gene and an antibiotic (e.g. spectinomycin) resistance gene, which allows selection in *B. subtilis*. Furthermore, it is required that the vector harbors restriction sites and does not replicate in *B. subtilis*. Similar as described for the generation of deletion vectors in this thesis, Wenzel and Altenbuchner (2015) cloned the flanking regions (about 700 bp) of the gene to be deleted into the vector. These flanking regions allowed integration of the vector into the *B. subtilis* chromosome due to a single cross-over event. The integration of the vector was positively selected for by growing the *B. subtilis* cells in the presence of spectinomycin. Subsequently, the selected cells were grown in the presence of mannose. When the cells have spontaneously lost the vector they are able to grow on a mannose containing medium. Afterwards, the colonies were grown on a spectinomycin containing medium to select for loss of the antibiotic resistance. Finally, spectinomycin sensitive colonies were screened for loss of the target gene region by colony PCR.

Wenzel and Altenbuchner (2015) reported that application of the presented method resulted in loss of the region of interest in 30 % to 70 % of the clones. The advantage of this method is the straightforward selection for the integration of the vector into the *B. subtilis* chromosome and the subsequent excision.

However, the clones can spontaneously loose the vector alone or jointly with the target gene. Therefore, extensive screening for loss of the target gene by colony PCR is necessary. Furthermore, the presented method also involves cloning of flanking regions of the target genes into a vector. However, Wenzel and Altenbuchner (2015) suggest additional methods of cloning flanking regions of the target genes into the vector, e.g. overlap extension PCR (Ho et al., 1989).

4.8. Labeling of ordered strains

The two fluorescent proteins GFP and mKATE were integrated into the chromosomes of the *B. subtilis* strains, which were obtained from the *Bacillus* genetic stock center. After transformation of the *B. subtilis* strains with the phy-GFP and phy-mKATE plasmids, the colored colonies indicated successful transformation. The starch hydrolysis test allowed selection of those transformants, where the GFP or mKATE sequence was integrated in the *amyE* gene of *B. subtilis*, as intended. However, the fluorescence of the transformants was not tested in e.g. a flow cytometer.

The ordered auxotrophic *B. subtilis* strains were generated differently than described in this study. *B. subtilis* 1A208, which is *hisH*$^-$, is auxotrophic for histidine. For the generation of the *B. subtilis* 1A208 strain, extracted DNA from the *B. subtilis* strain SB19 (original code) was transformed into the *B. subtilis* strain 1A58. *B. subtilis* strain 1A58 carries a mutation in the genes *hisH* and *trpC*, which was induced by UV treatment of the *B. subtilis* strain 168 (Nester and Lederberg, 1961). The gene product of *hisH* together with the gene product of *hisF* catalyzes the reaction to imidazole glycerol-3-phosphate, which is the sixth last step in the histidine biosynthesis pathway. However, imidazole glycerol-3-phosphate is also a precursor for the *de novo* purine biosynthesis. Therefore, inactivation of *hisH* might additionally have affected the *de novo* purine biosynthesis.

The ordered *B. subtilis* strains 1A543 (*trpC*$^-$), 1A553 (*trpA*$^-$), 1A560 (*trpB*$^-$), and 1A62 (*trpA*$^-$) were derived from the prototrophic *B. subtilis* strain 1A2. Mutations were induced by ultraviolet light, nitrosoguanidine, acridine half-mustards, nitrous acid, hydroxylamine, low pH, or ethyl methanesulfonate (Whitt and Carlton, 1968). The gene *trpC* was also chosen as target gene in this study. In contrast, the genes *trpA* and *trpB* encode the tryptophan synthase alpha chain and the tryptophan synthase beta chain.

The tryptophan synthase alpha- and beta chain together catalyze the reaction from (3-indoyl-) glycerolphosphate to tryptophan, whereas the tryptophan synthase alpha chain catalyzes the reaction from (3-indoyl-) glycerolphosphate to indole. Furthermore, the tryptophan synthase beta chain catalyzes the reaction from indole to tryptophan. However, a double deletion of *trpA* and *trpB* would be preferable, because each gene product alone might allow marginal biosynthesis of tryptophan.

Besides the *B. subtilis* strain 1A208, all ordered strains were exposed to mutagenic agents, which introduced point mutations and frameshift mutations, thus resulting in amino acid auxotrophies (Berg et al., 2002; Hoffmann et al., 1989; Hughes and Maloy, 2007; Malling and Serres, 1968; Ohnishi et al., 2008; Schaaper et al., 1987; Whitt and Carlton, 1968). In contrast, this study aimed for clean deletions of genes in *B. subtilis*, which were identified as target genes based on analysis of the amino acid biosynthesis pathways.

Similar as the *B. subtilis* strain 1A208 (*hisH*$^-$), the *B. subtilis* strains 1A543 (*trpC*$^-$), 1A553 (*trpA*$^-$), 1A560 (*trpB*$^-$), and 1A62 (*trpA*$^-$) were ultimately derived from *B. subtilis* 168 (Nester and Lederberg, 1961; Whitt and Carlton, 1968; Zeigler, 2000). However, *B. subtilis* 168 is a domestic laboratory strain, which lacks several characteristics of wild type *B. subtilis* strains, as described earlier in paragraph 1.4. (Zeigler et al., 2008). Therefore, comparison to nature would be more constraint with experiments with the *B. subtilis* strains 1A208, 1A543, 1A553, 1A560, and 1A62 than with *B. subtilis* NCIB 3610.

Due to time constraints, no coculture experiments with the labeled auxotrophic *B. subtilis* strains and amino acid overproducing *E. coli* strains could be performed. Therefore, the formation of nanotubes between amino acid auxotrophic *B. subtilis* strains and amino acid overproducing *E. coli* strains could not be analyzed in this study. However, it is likely that nanotubes are formed between these bacteria, because nanotubes were observed in cocultures containing amino acid overproducing *E. coli* (Pande et al., 2015) and between prototrophic *B. subtilis* and *E. coli* cells (Dubey and Ben-Yehuda, 2011).

4.9. Comparison of the studies by Dubey and Ben-Yehuda, (2011) and Pande et al., (2015)

In this paragraph, the studies of Dubey and Ben-Yehuda (2011) and Pande et al. (2015), which were briefly summarized in paragraph 1.3., will be compared. In both studies, naotubes were observed, which connected bacterial cells.

Dubey and Ben-Yehuda (2011) suggested that nanotubes consist of cell wall material and membrane compounds. Furthermore, they suggested that nanotubes contain outer and inner layers. This is partially in line with the study by Pande et al. (2015), which also suggests that nanotubes are composed of membrane derived lipids and that they are hollow. Due to the structural differences between the cell surface of Gram-negative and Gram-positive bacteria it is expected that also nanotubes structurally differ between the two types of bacteria. Indeed, Dubey and Ben-Yehuda (2011) observed differences between nanotubes formed by *E. coli*, which is Gram-negative and *B. subtilis*, which is Gram-positive. They reported that “the nanotubes formed by *E. coli* cells appeared significantly thinner than those formed by *B. subtilis*” (Dubey and Ben-Yehuda, 2011) There, the length of the nanotubes formed by *B. subtilis* was up to 1 µm and the width ranged from 30 nm to 130 nm. However, no average values characterizing the nanotubes formed by *E. coli* cells were reported. Pande et al. (2015) reported a length of nanotubes formed by *E. coli* ranging from 0.05 µm to 14 µm and an average width of 80 ± 10 nm. The comparison of these values however, does not support the observation that nanotubes formed by *E. coli* are thinner than those formed by *B. subtilis*. Future studies should analyze the differences between the nanotubes formed by Gram-nagtive and Gram-positive bacteria more exactly.

Notably, Dubey and Ben-Yehuda (2011) observed two different types of nanotubes formed by *B. subtils*. Besides larger nanotubes, they additionally observed smaller nanotubes, which closely connected nearby cells. Furthermore, they observed nanotubes emerging from different positions of the cell surface and that cells can be attached to more than one partner at the same time. The last two observations are in line with the study by Pande et al. (2015), however, there no different types of nanotubes formed by one organism were observed.

In both studies the transport of cytoplasmic compounds, such as proteins through nanotubes was observed. Moreover, Pande et al. (2015) suggested that also amino acids are transported in nanotubes. Interestingly, Dubey and Ben-Yehuda (2011) observed the transport of a plasmid (nonintegrative vector pHB201) through nanotubes. They suggested that nanotubes enable gene transfer between bacterial cells of the same or different species without the requirements in plasmid conjugation. There, the transport of plasmids between cells through conjugative pili is induced by genes located on the conjugative plasmid of the donor strains (Madigan et al., 2010). In contrast to plasmid conjugation, the transport of plasmids through nanotubes does not require particular donor and recipient cells. However, in the study of Pande et al. (2015) the plasmid pJBA24, which was used in the experiments, was not transferred between cells through nanotubes. They suggested that "the plasmid was bound to the host's chromosome and/or its inner membrane" (Pande et al., 2015). Furthermore, Dubey and Ben-Yehuda (2011) remarked that it is probable that bacteriophages can spread from cell to cell through nanotubes, however, this was not analyzed in their experiments. Both studies suggested that cytoplasmic compounds are transferred bidirectional through nanotubes on the population level. However, it remains unknown whether the transport is active or passive (Dubey and Ben-Yehuda, 2011).

It was expected that "static incubation of cocultures could facilitate cell-cell interactions" (Pande et al., 2015). Indeed, Dubey and Ben-Yehuda (2011) observed nanotubes connecting cells only when cocultures were cultivated on agarose pads. In this study, no nanotubes where observed when cocultures where grown in liquid medium. However, it was not documented whether the liquid cultures where incubated under shaking conditions. In contrast to this finding, Pande et al. (2015) observed no nanotube formation when cocultures where grown on agarose pads. There, cultivation of the cocultures in liquid medium with shaking conditions was required for the formation of nanotubes. They suggested that nanotubes inhibit active swimming of cells. However, it remains unknown what caused these different cultivation requirements for the formation of nanotubes in the two compared studies.

Besides the observation that nanotube formation is contact dependant, Pande et al. (2015) suggested that nanotube formation is triggered by nutrient starvation. This suggestion was based on the finding that nanontubes were only formed when the amino acid, which was required by the auxotrophic cross-feeding partner, was not

supplemented to the medium. They suggested that then the auxotrophic cells obtain the required amino acid from the amino acid overproducing cross-feeding partner through nanotubes. In contrast, no nanotubes were formed when the medium for the cross-feeding cocultures was supplemented with the amino acid, which was required by the auxotrophic cells. Furthermore, in this study it was required that cocultures were composed of amino acid overproducing cells (*E. coli* or *A. baylyi*) and *E. coli* cells, which were auxotrophic for the respective amino acid. Thus they suggested a regulatory mechanism for the formation of nanotubes depending on the nutritional status of the cell.

However, this is partly contradicted by the study of Dubey and Ben-Yehuda (2011), where numerous nanotubes were only observed when the cocultures were cultivated in a rich medium (LB medium). When cocultures were incubated on minimal medium, nanotubes were formed between cells but at lower frequency than when they were cultivated on rich medium. Notably, Dubey and Ben-Yehuda (2001) analyzed nanotube formation using prototrophic strains, which constrains drawing conclusions from the comparison of the two studies. Furthermore, experiments showed that nanotubes are formed by prototrophic *E. coli* in a low amount (Shitut, 2015). Nevertheless, Dubey and Ben-Yehuda (2011) observed nanotubes formed by prototrophic *E. coli*, *B. subtilis* and *S. aureus*. However, Dubey and Ben-Yehuda (2011) did not quantify nanotube formation in the cocultures. Thus it is not possible to state to what extend the study of Dubey and Ben-Yehuda (2011) contradicts the suggestion of Pande et al. (2015) that nanotube formation is triggered by nutrient starvation.

4.10. The impact of nanotubes

The nanotubes have several potential impacts on bacterial communities. For once, the study of Pande et al. (2015) suggests that amino acids are exchanged between cells through nanotubes in cross-feeding cultures. As explained in paragraph 1.2., it was suggested that 76 % of all Eubacteria are auxotrophic for one to 25 metabolites (D'Souza et al., 2014). Thus it is likely that nanotube formation is a common mechanism in bacteria to endure nutrition starvation. This assumption is supported by the observation of nanotubes in Gram negative bacteria as well as in Gram positive bacteria (Dubey and Ben-Yehuda, 2011).

However, in the study of Pande et al. (2015) it was observed that *A. baylyi* does not form nanotubes. This indicates that not all bacteria have the genes, which are required for nanotube formation. Currently, the required genes for nanotube formation are not identified however.

Interestingly, one bacterial cell can be attached to more than one other bacterial cell using nanotubes so that intercellular networks are formed, where cytoplasmic compounds, such as metabolites and proteins are exchanged between cells. As a result, bacterial communities might “function as multicellular, interconnected entities rather than as individual, physiologically autonomous unities” (Pande et al., 2015). This might be one reason why more than 99 % of bacteria species are not culturable in the laboratory (Madigan et al., 2010). Notably, the formation of nanotubes and the exchange of cytoplasmic compounds could potentially be performed in different ecological interactions ranging from parasitic to mutualistic interactions (Pande et al., 2015).

Furthermore, Dubey and Ben-Yehuda (2011) suggested that the exchange of cytoplasmic compounds between bacterial cells of the same or different species through nanotubes might represent a possible way of bacterial communication. They speculate that signaling molecules would be protected from degrading enzymes and severe environmental conditions when they are transported in nanotubes. However, bacterial communication involves sending of a signal and a response to that signal by changed gene expression (Keller and Surette, 2006). Furthermore, it is not known how specific the transport of molecules through nanotubes is. Therefore, the suggestion that nanotubes provide a potential way of bacterial communication remains speculation.

5. CONCLUSION

The aim of this study was to generate amino acid auxotrophic *B. subtilis* strains, with which the formation of nanotubes should be analyzed. However, when *B. subtilis* was transformed with the generated deletion vectors and LFH-PCR products, no auxotrophic transformants were obtained. This implies that different methods should be applied to generate auxotrophic *B. subtiis* strains in similar future studies, e.g. the gene deletion method, which uses mannose resistance or sensitivity as described by Wenzel and Altenbuchner (2015).

The labeled auxotrophic *B. subtilis* strains can be used for future experiments. However, they might not be appropriate for long-term evolution experiments. *B. subtilis* is capable of natural transformation, which is a “genetically programmed mechanism for horizontal gene transfer in bacteria” (Mortier-Barrière et al., 2007). Therefore, auxotropic *B. subtilis* strains might revert to prototrophic strains, due to natural transformation in long-term experiments. This would especially be a problem with the *B. subtilis* strains, which were generated with mutagenic agents. Since these *B. subtilis* strains are auxotrophic only due to point mutations or frameshift mutations, they might revert quickly to prototrophic strains in long-term experiments.

Several open questions about the characteristics of nanotubes remain, which should be addressed in future studies. On the one hand, the exact structure of the nanotubes remains unknown as well as the differences between nanotubes of Gram negative and Gram positive bacteria. On the other hand, more experiments have to show what compounds are exchanged between cells through nanotubes. It remains unknown to what extent genetic material is transported through nanotubes. The exchange of plasmids between cells through nanotubes also has medical implications when the plasmids encode antibiotic resistance proteins. This is of medical importance because of the emergence of drug-specific resistances in disease causing bacteria, where treatment of the disease with existent drugs is not possible (Madigan et al., 2010). Furthermore, Dubey and Ben-Yehuda (2011) pointed out the possibility that commensal bacteria could support the growth of pathogenic bacteria by exchange of nutrients through nanotubes.

Further remaining open questions are how specific the transport through nanotubes is and whether the transport is active or passive. Additionally, more experiments are necessary to investigate whether nanotube formation is indeed triggered by nutrient starvation because this is partly contradicted by the study of Dubey and Ben-Yehuda (2001). Furthermore, it remains unknown whether chemosensory mechanisms are involved in nanotube formation for the identification of potential target cells, or whether it is arbitrary. Moreover, future studies could identify the required genes for nanotube formation. Another question is what caused the differences in required cultivation conditions for nanotube formation between the compared studies by Dubey and Ben-Yehuda (2001) and Pande et al. (2015). Finally, future studies could investigate what impact nanotubes have in parasitic interactions in contrast to mutualistic interactions in bacterial communities.

6. REFERENCES

Altschul, S.F., Gish, W., Miller, W., Myers, E.W., and Lipman, D.J. (1990). Basic Local Alignment Search Tool. J. Mol. Biol. *215*, 403–410.

Avila-Calderón, E.D., Araiza-Villanueva, M.G., Cancino-Diaz, J.C., López-Villegas, E.O., Sriranganathan, N., Boyle, S.M., and Contreras-Rodríguez, A. (2015). Roles of bacterial membrane vesicles. Arch. Microbiol. *197*, 1–10.

Begon, M., Harper, J.L., and Townsend, C.R. (1996). Ecology. Individuals, Populations and Communities (Berlin, Germany: Blackwell Wissenschafts-Verlag).

Berg, J.M., Tymoczko, J.L., and Stryer, L. (2002). Biochemistry (New York: W H Freeman).

Bertels, F., Merker, H., and Kost, C. (2012). Design and Characterization of Auxotrophy-Based Amino Acid Biosensors. PLoS One *7*, e41349.

Beveridge, T.J. (1999). Structures of Gram-Negative Cell Walls and Their Derived Membrane Vesicles. J. Bacteriol. *181*, 4725–4733.

Birnboim, H.C., and Doly, J. (1979). A rapid alkaline extraction procedure for screening recombinant DNA. Nucleic Acids Res. *7*, 1513–1524.

Boyer, M., and Wisniewski-Dyé, F. (2009). Cell-cell signalling in bacteria: not simply a matter of quorum. FEMS Microbiol. Ecol. *70*, 1–19.

Brown, L., Kessler, A., Cabezas-Sanchez, P., Luque-Garcia, J.L., and Casadevall, A. (2014). Extracellular vesicles produced by the Gram-positive bacterium *Bacillus subtilis* are disrupted by the lipopeptide surfactin. Mol. Microbiol. *93*, 183–198.

Butcher, R. a, Schroeder, F.C., Fischbach, M. a, Straight, P.D., Kolter, R., Walsh, C.T., and Clardy, J. (2007). The identification of bacillaene, the product of the PksX megacomplex in *Bacillus subtilis*. Proc. Natl. Acad. Sci. U. S. A. *104*, 1506–1509.

Caspi, R., Altman, T., Billington, R., Dreher, K., Foerster, H., Fulcher, C.A., Holland, T.A., Keseler, I.M., Kothari, A., Kubo, A., et al. (2014). The MetaCyc database of metabolic pathways and enzymes and the BioCyc collection of Pathway/Genome Databases. Nucleic Acids Res. *42*, D459–D471.

Cleavage Close to the End of DNA Fragments. New England BioLabs. https://www.neb.com/tools-and-resources/usage-guidelines/cleavage-close-to-the-end-of-dna-fragments [27.04.2015].

D'Souza, G., Waschina, S., Pande, S., Bohl, K., Kaleta, C., and Kost, C. (2014). Less is more: selective advantages can explain the prevalent loss of biosynthetic genes in bacteria. Evolution (N. Y). *68*, 2559–2570.

Dubey, G.P., and Ben-Yehuda, S. (2011). Intercellular Nanotubes Mediate Bacterial Communication. Cell *144*, 590–600.

Dubnau, D. (1993). Genetic exchange and homologous recombination in *Bacillus subtilis* and Other Gram-Positive Bacteria; Biochemistry, Physiology, and Molecular Genetics, R. Losick, ed. (Washington, DC: American Society for Microbiology), pp. 555–584.

Ducret, A., Fleuchot, B., Bergam, P., and Mignot, T. (2013). Direct live imaging of cell–cell protein transfer by transient outer membrane fusion in Myxococcus xanthus. Elife *2*, e00868.

Faires, N., Tobisch, S., Bachem, S., Martin-Verstraete, I., Hecker, M., and Stülke, J. (1999). The Catabolite Control Protein CcpA Controls Ammonium Assimilation in *Bacillus subtilis*. J. Mol. Microbiol. Biotechnol. *1*, 141–148.

Faust, K., and Raes, J. (2012). Microbial interactions: from networks to models. Nat. Rev. Microbiol. *10*, 538–550.

Freilich, S., Zarecki, R., Eilam, O., Segal, E.S., Henry, C.S., Kupiec, M., Gophna, U., Sharan, R., and Ruppin, E. (2011). Competitive and cooperative metabolic interactions in bacterial communities. Nat. Commun. *2*, DOI: 10.1038/ncomms1597.

Gallegos-Monterrosa, R. (2015). Personal communication.

Gallegos-Monterrosa, R., unpublished.

van Gestel, J., Weissing, F.J., Kuipers, O.P., and Kovács, Á.T. (2014). Density of founder cells affects spatial pattern formation and cooperation in *Bacillus subtilis* biofilms. ISME J. *8*, 2069–2079.

Glasel, J.A. (1995). Validity of nucleic acid purities monitored by 260nm/280nm absorbance ratios. Biotechniques *18*, 62–63.

Hamoen, L.W., Venema, G., and Kuipers, O.P. (2003). Controlling competence in *Bacillus subtilis*: shared use of regulators. Microbiology *149*, 9–17.

Hanahan, D. (1983). Studies on Transformation of *Escherichia coli* with Plasmids. J. Mol. Biol. *166*, 557–580.

Harcombe, W. (2010). Novel cooperation experimentally evolved between species. Evolution (N. Y). *64*, 2166–2172.

Hayes, C.S., Aoki, S.K., and Low, D.A. (2010). Bacterial Contact-Dependent Delivery Systems. Annu. Rev. Genet. *44*, 71–90.

Ho, S.N., Hunt, H.D., Horton, R.M., Pullen, J.K., and Pease, L.R. (1989). Site-directed mutagenesis by overlap extension using the polymerase chain reaction. Gene *77*, 51–59.

Hoffmann, G.R., Freemer, C.S., and Parente, L.A. (1989). Induction of genetic duplications and frameshift mutations in *Salmonella typhimurium* by acridines and acridine mustards : Dependence on covalent binding of the mutagen to DNA. Mol. Genet. Genomics *218*, 377–383.

Hölscher, T., Bartels, B., Lin, Y.-C., Gallegos-Monterrosa, R., Price-Whelan, A., Kolter, R., Dietrich, L.E.P., and Kovács, Á.T. (2015). Motility, Chemotaxis and Aerotaxis Contribute to Competitiveness during Bacterial Pellicle Biofilm Development. J. Mol. Biol. *427*, 3695–3708.

Hughes, K.T., and Maloy, S.R. (2007). Advanced Bacterial Genetics: Use of Transposons and Phage for Genomic Engineering: 421 (Methods in Enzymology) (Academic Press).

iGEM Groningen. *B. subtilis* transformation. http://2013.igem.org/Team:Groningen/protocols/Transformation [05.08.2015].

Kanehisa, M., Goto, S., Sato, Y., Kawashima, M., Furumichi, M., and Tanabe, M. (2014). Data, information, knowledge and principle: back to metabolism in KEGG. Nucleic Acids Res. *42*, D199–D205.

Kearns, D.B., Chu, F., Rudner, R., and Losick, R. (2004). Genes governing swarming in *Bacillus subtilis* and evidence for a phase variation mechanism controlling surface motility. Mol. Microbiol. *52*, 357–369.

Kearse, M., Moir, R., Wilson, A., Stones-Havas, S., Cheung, M., Sturrock, S., Buxton, S., Cooper, A., Markowitz, S., Duran, C., et al. (2012). Geneious Basic: An integrated and extendable desktop software platform for the organization and analysis of sequence data. Bioinformatics *28*, 1647–1649.

Keller, L., and Surette, M.G. (2006). Communication in bacteria: an ecological and evolutionary perspective. Nat. Rev. Microbiol. *4*, 249–258.

Kinsinger, R.F., Shirk, M.C., and Fall, R. (2003). Rapid surface motility in *Bacillus subtilis* is dependent on extracellular surfactin and potassium ion. J. Bacteriol. *185*, 5627–5631.

Konkol, M. a., Blair, K.M., and Kearns, D.B. (2013). Plasmid-Encoded ComI Inhibits Competence in the Ancestral 3610 Strain of *Bacillus subtilis*. J. Bacteriol. *195*, 4085–4093.

Koressaar, T., and Remm, M. (2007). Enhancements and modifications of primer design program Primer3. Bioinformatics *23*, 1289–1291.

Krauss, U., Eggert, T. (2015). Ligation Calculator. In.silico. Online Bioiinformatics Resources. http://www.insilico.uni-duesseldorf.de/Lig_Input.html [06.06.2015].

Lal, A., and Cheeptham, N. Starch Agar Protocol. Microbe Library. http://www.microbelibrary.org/library/laboratory-test/3780-starch-agar-protocol [20.11.2015].

Lambert, J.M., Bongers, R.S., and Kleerebezem, M. (2007). Cre-*lox*-Based System for Multiple Gene Deletions and Selectable-Marker Removal in *Lactobacillus plantarum*. Appl. Environ. Microbiol. *73*, 1126–1135.

Leboffe, M.J., and Pierce, B.E. (2010). Microbiology: Laboratory Theory and Application (Englewood, USA: Morton Publishing Company).

Lee, E.Y., Choi, D.Y., Kim, D.K., Kim, J.W., Park, J.O., Kim, S., Kim, S.H., Desiderio, D.M., Kim, Y.K., Kim, K.P., et al. (2009). Gram-positive bacteria produce membrane vesicles: Proteomics-based characterization of *Staphylococcus aureus*-derived membrane vesicles. Proteomics *9*, 5425–5436.

Madigan, M.T., Martinko, J.M., Stahl, D.A., and Clark, D.P. (2010). Brock. Biology of Microorganisms (San Francisco: Pearson Education).

Malling, H., and Serres, F. De (1968). Identification of Genetic alterations induced by Ethyl methanesulfonate in *Neurospora crassa*. Mutat. Res. *6*.

Mashburn, L.M., and Whiteley, M. (2005). Membrane vesicles traffic signals and facilitate group activities in a prokaryote. Nature *437*, 422–425.

McLoon, A.L., Guttenplan, S.B., Kearns, D.B., Kolter, R., and Losick, R. (2011). Tracing the Domestication of a Biofilm-Forming Bacterium. J. Bacteriol. *193*, 2027–2034.

Mortier-Barrière, I., Velten, M., Dupaigne, P., Mirouze, N., Piétrement, O., McGovern, S., Fichant, G., Martin, B., Noirot, P., Le Cam, E., et al. (2007). A key presynaptic role in transformation for a widespread bacterial protein: DprA conveys incoming ssDNA to RecA. Cell *130*, 824–836.

Mullineaux, C.W., Mariscal, V., Nenninger, A., Khanum, H., Herrero, A., Flores, E., and Adams, D.G. (2008). Mechanism of intercellular molecular exchange in heterocyst-forming cyanobacteria. EMBO J. *27*, 1299–1308.

Munk, K., Dersch, P., Eikmanns, B., Eikmanns, M., Fischer, R., Jahn, D., Jahn, M., Nethe-Jaenchen, R., Requena, N., and Schultze, B. (2008). Mikrobiologie (Stuttgart: Thieme Verlag).

NEB. Rubidium Chloride Method. https://www.neb.com/nebecomm/tech_reference/gene_expression/RbChlorideMethod [page expired].

Nester, B.Y.E.W., and Lederberg, J. (1961). Linkage of genetic units of *Bacillus subtilis* in DNA transformation. Proc. Natl. Acadamy Sci. United States Am. *47*, 52–55.

Odgen, R.C., and Adamy, D.A. (1987). Electrophoresis in Agarose and Acrylamid Gels. Methods Enzymol. *152*, 61–87.

Ohnishi, J., Mizoguchi, H., Takeno, S., and Ikeda, M. (2008). Characterization of mutations induced by N-methyl-N'-nitro-N-nitrosoguanidine in an industrial *Corynebacterium glutamicum* strain. Mutat. Res. *649*, 239–244.

Pande, S., Merker, H., Bohl, K., Reichelt, M., Schuster, S., de Figueiredo, L.F., Kaleta, C., and Kost, C. (2014). Fitness and stability of obligate cross-feeding interactions that emerge upon gene loss in bacteria. ISME J. *8*, 953–962.

Pande, S., Shitut, S., Freund, L., Westermann, M., Bertels, F., Colesie, C., Bischofs, I.B., and Kost, C. (2015). Metabolic cross-feeding via intercellular nanotubes among bacteria. Nat. Commun. *6*, 6238.

Rastogi, V.B., and Kishore, B. (2006). A Complete Course in ISC Biology. Volume 1 (New Delhi, India: Pitambar Publishing).

Sachs, J.L. (2006). Cooperation within and among species. J Evol Biol *19*, 1415–1436.

Sachs, J.L., Mueller, U.G., Wilcox, T.P., and Bull, J.J. (2004). The evolution of cooperation. Q. Rev. Biol. *79*, 135–160.

Safety data sheet. Kanamycin sulfate. Carl-Roth. https://www.carlroth.com/downloads/sdb/en/T/SDB_T832_GB_EN.pdf [25.01.2016].

Sauer, B. (1987). Functional Expression of the cre-lox Site-Specific Recombination System in the Yeast *Saccharomyces cerevisiae*. Mol. Cell. Biol. *7*, 2087–2096.

Schaaper, R.M., Dunn, R.L., and Glickman, B.W. (1987). Mechanisms of Ultraviolet-induced Mutation. Mutational Spectra in the *Escherichia coli lacI* gene for a Wild-type and an Excision-Repair-deficient Strain. J. Mol. Biol. *198*, 187–202.

Seth, E.C., and Taga, M.E. (2014). Nutrient cross-feeding in the microbial world. Front. Microbiol. *5*, doi:10.3389/fmicb.2014.00350.

Star activity. New England BioLabs.

https://www.neb.com/tools-and-resources/usageguidelines/star-activity [23.01.2016].

Shitut, S. (2015). Personal communication.

SubtiWiki. http://subtiwiki.uni-goettingen.de/bank/index.php?gene=hisD&action=Go [25.01.2016; a].

SubtiWiki. http://subtiwiki.uni-goettingen.de/bank/index.php?gene=thrc&action=Go [25.01.2016; b].

Suzuki, N., Nonaka, H., Tsuge, Y., Inui, M., and Yukawa, H. (2005). New Multiple-Deletion Method for the *Corynebacterium glutamicum* Genome, Using a Mutant lox Sequence. Microbiology *71*, 8472–8480.

T_m calculator. https://www.thermofisher.com/de/de/home/brands/thermo-scientific/molecular-biology/molecular-biology-learning-center/molecular-biology-resource-library/thermo-scientific-web-tools/tm-calculator.html [27.04.2015].

Untergasser, A., Cutcutache, I., Koressaar, T., Ye, J., Faircloth, B.C., Remm, M., and Rozen, S.G. (2012). Primer3-new capabilities and interfaces. Nucleic Acids Res. *40*, e115.

Vogelstein, B., and Gillespie, D. (1979). Preparative and analytical purification of DNA from agarose. Proc. Natl. Acad. Sci. U. S. A. *76*, 615–619.

Vos, P., Garrity, G., Jones, D., Krieg, N.R., Ludwig, W., Rainey, F.A., Schleifer, K.-H., and Whitman, W. (2009). Bergey's Manual of Systematic Bacteriology Volume 3: The Firmicutes (New York: Springer-Verlag).

Wenzel, M., and Altenbuchner, J. (2015). Development of a markerless gene deletion system for *Bacillus subtilis* based on the mannose phosphoenolpyruvate-dependent phosphotransferase system. Microbiology *161*, 1942–1949.

Wenzel, M., Müller, A., Siemann-Herzberg, M., and Altenbuchner, J. (2011). Self-inducible *Bacillus subtilis* Expression System for Reliable and Inexpensive Protein Production by High-Cell-Density Fermentation. Appl. Environ. Microbiol. *77*, 6419–6425.

Wertman, K.F., Wyman, A.R., and Botstein, D. (1986). Host/vector interactions which affect the viability of recombinant phage lambda clones. Gene *49*, 253–262.

Whitt, D.D., and Carlton, B.C. (1968). Characterization of Mutants with Single and Multiple Defects in the Tryptophan Biosynthetic Pathway in *Bacillus subtilis*. J. Bacteriol. *96*, 1273–1280.

Wink, M. (2006). An Introduction to Molecular Biotechnology (Weinheim: John Wiley & Sons).

Wright, G.D., and Thompson, P.R. (1999). Aminoglycoside phosphotransferases: Proteins, structure, and mechanism. Fronities Biosci. *4*, 9–22.

Yan, X., Yu, H.-J., Hong, Q., and Li, S.-P. (2008). Cre/*lox* System and PCR-Based Genome Engineering in *Bacillus subtilis*. Appl. Environ. Microbiol. *74*, 5556–5562.

Zeigler, D.R. (2000). Bacillus Genetic Stock Center Catalog of Strains, Seventh Edition, Volume 1: *Bacillus subtilis* 168. 1–71.

Zeigler, D.R., Pragai, Z., Rodriguez, S., Chevreux, B., Muffler, A., Albert, T., Bai, R., Wyss, M., and Perkins, J.B. (2008). The Origins of 168, W23, and Other *Bacillus subtilis* Legacy Strains. J. Bacteriol. *190*, 6983–6995.

7. SUPPLEMENTARY

Table S1: FastDigest restriction enzymes used for double-digestion of the amplified flanking regions of the target genes and the respective incubation times for the gene deletion with a vector.

PCR product	FastDigest restriction enzyme	Incubation time (in min)			
		A1	A2	A3	A4
argH downstream region	*Sal*I	80	100	100	90
	*Eco*RI	30	30	30	90
argH upstream region	*Sac*I	-	-	90	90
	*Xba*I	-	-	30	90
hisD downstream region	*Hind*III	40	60	60	90
	*Eco*RI	30	30	30	90
hisD upstream region	*Sac*I	-	-	90	90
	*Xba*I	-	-	30	90
lysA downstream region	*Hind*III	40	60	60	90
	*Eco*RI	30	30	30	90
lysA upstream region	*Sac*I	-	-	90	90
	*Xba*I	-	-	30	90
tyrA downstream region	*Sal*I	80	100	100	90
	*Eco*RI	30	30	30	90
tyrA upstream region	*Sac*I	-	-	90	90
	*Xba*I	-	-	30	90
pheA downstream region	*Hind*III	40	60	60	90
	*Eco*RI	30	30	30	90
pheA upstream region	*Sac*I	-	-	90	90
	*Xba*I	-	-	30	90
trpC downstream region	*Hind*III	40	60	60	90
	*Eco*RI	30	30	30	90
trpC upstream region	*Sac*I	-	-	90	90
	*Xba*I	-	-	30	90
thrC downstream region	*Hind*III	40	60	90	90
	*Pst*I	60	30	30	90
thrC upstream region	*Bam*HI	-	-	30	90
	*Not*I	-	-	30	90

Table S2: FastDigest restriction enzymes used for double-digestion of the plasmids pTB120 *lox*-Neo-*lox*, pTB233 *lox*-Sp-*lox* and pTB233 *lox*-Sp-*lox* with the inserted downstream flanking regions of the target genes and the respective incubation times for the gene deletion with a vector.

	FastDigest	**Incubation time (in min)**			
	restriction enzyme	A1	A2	A3	A4
pTB120 *lox*-Neo-*lox* / pTB233 *lox*-Sp-*lox*	*Sal*I	30	60	60	90
	*Eco*RI	30	30	30	90
pTB120 *lox*-Neo-*lox* / pTB233 *lox*-Sp-*lox*	*Hind*III	30	60	60	90
	*Eco*RI	30	30	30	90
pTB120 *lox*-Neo-*lox* / pTB233 *lox*-Sp-*lox*	*Hind*III	30	60	60	90
	*Pst*I	30	30	30	90
pTB233 *lox*-Sp-*lox* with inserted	*Xba*I	-	-	30	90
downstream flanking region	*Sac*I	-	-	60	90
pTB233 *lox*-Sp-*lox* with inserted	*Bam*HI	-	-	30	90
downstream flanking region	*Not*I	-	-	100	90

Table S3: Components of the double-digestion reactions for testing whether the flanking regions of the target genes were cloned into the plasmid pTB120 *lox*-Neo-*lox* or pTB233 *lox-Sp-lox.*

Compound	**Volume (µl)**
Plasmid DNA	5
FastDigest buffer	2
FastDigest restriction enzyme	1 of each
ddH_2O	11

Table S4: Components of the digestion reaction for plasmids pTB233 *lox*-Sp-*lox* with inserted flanking regions of *hisD* and *thrC.*

Compound	**Volume (µl)**
Plasmid DNA	5
10 x FastDigest Buffer	4
FastDigest *Sca*I	4
ddH2O	27

Table S5: Sequences of the primers for the amplification of the flanking regions of the target genes for the LFH-PCR. The *lox*-site 66 is marked in red and the *lox* site 71 is marked in green.

Amino acid	Primer name	Gene region	*lox* site added	Sequence (5‘ to 3‘)
arginine	1_LFH_d_fw	*argH* ds.	no	AAGTCGATCCTTCCGAAGCG
	1_LFH_d_rv	*argH* ds.	*lox*66	ATAACTTCGTATAGCATACATTATACGAA CGGTACACCGGATTCAAACAGGTGG
	1_LFH_u_fw	*argH* us.	*lox*71	ATAACTTCGTATAATGTATGCTATACGAA CGGTACGGATTTTCAACTCTTCTTCTGC
	1_LFH_u_rv	*argH* us.	no	TGACGGTGTTTCCTACTCGC
histidine	2_LFH_d_fw	*hisD* ds.	no	CGCCGATCATTTACAGCATCC
	2_LFH_d_rv	*hisD* ds.	*lox*66	ATAACTTCGTATAGCATACATTATACGAA CGGTAAGCCTTTGAAGAACATGCCG
	2_LFH_u_fw	*hisD* us.	*lox*71	ATAACTTCGTATAATGTATGCTATACGAA CGGTAAAATTTCGCCGTGTAGCTGC
	2_LFH_u_rv	*hisD* us.	no	GGATGTCATGCTGGAGGAGG
lysine	3_LFH_d_fw	*lysA* ds.	no	CAGCCGGTGTTAAAGATGCG
	3_LFH_d_rv	*lysA* ds.	*lox*66	ATAACTTCGTATAGCATACATTATACGAA CGGTATTTGTCGAAAACGGTGAGGC
	3_LFH_u_fw	*lysA* us.	*lox*71	ATAACTTCGTATAATGTATGCTATACGAA CGGTATAGAGAGCATCCACACCTCC
	3_LFH_u_rv	*lysA* us.	no	GCATATCCCGATCATCCTGC
tyrosine	4_LFH_d_fw	*tyrA* ds.	no	GGTCCCGAGATTTATGGGGC
	4_LFH_d_rv	*tyrA* ds.	*lox*66	ATAACTTCGTATAGCATACATTATACGAA CGGTAGCATCAGTATCACGAATATCCGC
	4_LFH_u_fw	*tyrA* us.	*lox*71	ATAACTTCGTATAATGTATGCTATACGAA CGGTATTCCGATAATCCGTTTGCCG
	4_LFH_u_rv	*tyrA* us.	no	CGGAATTGCTGACGAGAACC
phenylalanine	5_LFH_d_fw	*pheA* ds.	no	AAATCACCGCTGACAGGAGG
	5_LFH_d_rv	*pheA* ds.	*lox*66	ATAACTTCGTATAGCATACATTATACGAA CGGTAATTGATTCCAGGGGCCATGC
	5_LFH_u_fw	*pheA* us.	*lox*71	ATAACTTCGTATAATGTATGCTATACGAA CGGTAGTAAGCAACATGTTCGGCGC
	5_LFH_u_rv	*pheA* us.	no	CGGAATGGGTGTTGATGAAGC
tryptophan	6_LFH_d_fw	*trpC* ds.	no	TAGGCGTGTGATGCTATCCG
	6_LFH_d_rv	*trpC* ds.	*lox*66	ATAACTTCGTATAGCATACATTATACGAA CGGTATTGTCAATGAACATGGGGCG
	6_LFH_u_fw	*trpC* us.	*lox*71	ATAACTTCGTATAATGTATGCTATACGAA CGGTACAGCGCCTCCTTAAATGAACG
	6_LFH_u_rv	*trpC* us.	no	GCGCTGATGTTTTAGAGGAGC
threonine	7_LFH_d_fw	*thrC* ds.	no	TCCTTGGACATGATCGCAGC
	7_LFH_d_rv	*thrC* ds.	*lox*66	ATAACTTCGTATAGCATACATTATACGAA CGGTACTGAAAGATCCGAACACAGCG
	7_LFH_u_fw	*thrC* us.	*lox*71	ATAACTTCGTATAATGTATGCTATACGAA CGGTAGCCTTCCGTTTTGACATGAAGC
	7_LFH_u_rv	*thrC* us.	no	TGCTTCCTGACCATCATCCG

ds.: downstream. us.: upstream. fw: forward. rv: reverse.

Table S6: Primers for the amplification of the kanamycin- and spectinomycin resistance cassette for the LFH-PCR. The primers were obtained from the Junior Research Group Terrestrial Biofilms in Jena.

Resistance cassette for	Primer name	Added *lox*-site	Sequence (5' to 3')
kanamycin	oRGM7 (fw)	*lox*71	TACCGTTCGTATAGCATACATTATACGAAG TTATTAGAGCTTGGGTTACAGGCATGG
	oRGM2 (rv)	*lox*66	TACCGTTCGTATAATGTATGCTATACGAAG TTATAGATCAATTTGATAATTACTAATAC
spectinomycin	oRGM16 (fw)	*lox*71	TACCGTTCGTATAGCATACATTATACGAAG TTATCTCGAGATCCCCCTATGCAAGGG
	oRGM17 (rv)	*lox*66	TACCGTTCGTATAATGTATGCTATACGAAG TTATTAAAAAATTTAGAAGCCAATGAAATC

The *lox*-site 66 is marked in red and the *lox* site 71 is marked in green. fw: forward. rv: reverse

Table S7: Amplified gene regions with the respective positions in the *B. subtilis* genome for the generation of template DNA for the LFH-PCR.

Gene region	Position in *B. subtilis* genome
argH	3014087 - 3010855
hisD	3588169 - 3585565
lysA	2438948 - 2436347
tyrA	2370968 - 2368514
pheA	2852882 - 2850640
trpC	2375746 - 2373468
thrC	3315495 - 3313036

Table S8: Compounds for the digestion reaction with the FastDigest restriction enzyme *Kpn*I (Thermo Fisher Scientific).

Compound	Voume (µl)
Colony PCR product	10
10 x FastDigest Buffer	3
FastDigest enzyme *Kpn*I	3
ddH2O	14

Table S9: Incorrect primers used for sequencing of the LFH-PCR products. The *lox*-sites were added with incorrect orientation to the 5' ends of the primers.

Amino acid	Primer name	Gene-region	*lox* site added	Sequence (5' to 3')
arginine	1_LFH_d_fw	*argH* ds.	no	AAGTCGATCCTTCCGAAGCG
	1_LFH_d_rv	*argH* ds.	*lox*66	TACCGTTCGTATAATGTATGCTATACGAA GTTATCACCGGATTCAAACAGGTGG
	1_LFH_u_fw	*argH* us.	*lox*71	TACCGTTCGTATAGCATACATTATACGAA GTTATCGGATTTTCAACTCTTCTTCTGC
	1_LFH_u_rv	*argH* us.	no	TGACGGTGTTTCCTACTCGC
lysine	3_LFH_d_fw	*lysA* ds.	no	CAGCCGGTGTTAAAGATGCG
	3_LFH_d_rv	*lysA* ds.	*lox*66	TACCGTTCGTATAATGTATGCTATACGAA GTTATTTTGTCGAAAACGGTGAGGC
	3_LFH_u_fw	*lysA* us.	*lox*71	TACCGTTCGTATAGCATACATTATACGAA GTTATTAGAGAGCATCCACACCTCC
	3_LFH_u_rv	*lysA* us.	no	GCATATCCCGATCATCCTGC

ds.: downstream. us.: upstream. fw: forward. rv: reverse

Danksagung

Ich möchte Dr. Kost und Prof. Dr. Wöstemeyer für die Betreuung dieser Masterarbeit danken. Außerdem danke ich den Mitgliedern der Gruppe Experimentelle Ökologie und Evolution, namentlich Anne-Kathrin Dietel, Samir Giri, Glen D'Souza, Shraddha Shitut, Ghada Mohamed Yousif Abdelsalam, Daniel Preußger, Silvio Waschina, Muhammad Atiqur Rahman, Elena Inguglia und Esther Voigt. Sie haben immer Zeit gefunden, mir im Labor zu helfen oder die Experimente zu planen und zu diskutieren. Im Besonderen danke ich Ramses Gallegos Monterrosa von der Gruppe Terrestrische Biofilme in Jena für die ausführlichen Besprechungen der Experimente und die Unterstützung im dortigen Labor. Ein großer Dank gilt zuletzt meinen Freunden und meiner Familie, die mich durch diese Zeit begleitet haben. Dabei möchte ganz besonders meinem Freund danken, der immer für mich da war, mir immer wieder auf die Beine geholfen hat und eine große Stütze in dieser Zeit war.

Selbstständigkeitserklärung

Hiermit versichere ich, dass ich die vorliegende Arbeit selbstständig verfasst und keine anderen als die angegebenen Quellen und Hilfsmittel benutzt habe, alle Ausführungen, die anderen Schriften wörtlich oder sinngemäß entnommen wurden, kenntlich gemacht sind und die Arbeit in gleicher oder ähnlicher Fassung noch nicht Bestandteil einer Studien – oder Prüfungsleistung war.